

# *beowulf* technical notes

Davison E. Soper

*Institute of Theoretical Science, University of Oregon  
Eugene, OR 97403, USA*

## Abstract

These notes provide a technical description of the algorithms used in the program *beowulf*, which computes infrared safe three-jet-like observables in electron-positron annihilation at next to leading order in Quantum Chromodynamics.

Notes: 23 March 2001  
*beowulf* version 1.1

## 1 Introduction

Consider an infrared safe observable of the form

$$\begin{aligned} \sigma = & \frac{1}{2!} \int d\vec{k}_1 d\vec{k}_2 \frac{d\sigma_2}{d\vec{k}_1 d\vec{k}_2} \mathcal{S}_2(\vec{k}_1, \vec{k}_2) \\ & + \frac{1}{3!} \int d\vec{k}_1 d\vec{k}_2 d\vec{k}_3 \frac{d\sigma_3}{d\vec{k}_1 d\vec{k}_2 d\vec{k}_3} \mathcal{S}_3(\vec{k}_1, \vec{k}_2, \vec{k}_3) \\ & + \frac{1}{4!} \int d\vec{k}_1 d\vec{k}_2 d\vec{k}_3 d\vec{k}_4 \frac{d\sigma_4}{d\vec{k}_1 d\vec{k}_2 d\vec{k}_3 d\vec{k}_4} \mathcal{S}_4(\vec{k}_1, \vec{k}_2, \vec{k}_3, \vec{k}_4). \end{aligned} \quad (1)$$

Here the  $d\sigma_n$  are the order  $\alpha_s^2$  contributions to the parton level cross section. Each contains momentum and energy conserving delta functions. The  $d\sigma_n$  include ultraviolet renormalization in the  $\overline{\text{MS}}$  scheme. The functions  $\mathcal{S}$  describe the measurable quantity to be calculated. The normalization is such that  $\mathcal{S}_n = 1$  for  $n = 2, 3, 4$  would give the order  $\alpha_s^2$  perturbative contribution the the total cross section. There are, of course, infrared divergences associated with Eq. (1). We will discuss these in great detail, but for now, we may simply suppose that an infrared cutoff has been supplied.

We suppose that  $\sqrt{s} \gg m_j$  for any of the quark masses  $m_j$  and that  $\sqrt{s}$  is also large compared to a generic hadron mass  $m$ . We also suppose that the measurement, as specified by the functions  $\mathcal{S}_n$ , is infrared safe, as described in Kunszt and Soper [KS]. This implies that  $\sigma$  is not sensitive to any infrared scales  $m$ . In particular, we can perform the calculation with all quark masses set to zero.

We wish to calculate a “three-jet” quantity. That is,  $\mathcal{S}_2 = 0$ . Furthermore, this quantity should be dimensionless. It is convenient to take the functions  $\mathcal{S}_n$  to be dimensionless and to eliminate the remaining dimensionality in the problem by dividing by  $\sigma_0$ , the total  $e^+e^-$  cross section at the Born level. Thus, for instance,  $\sigma/\sigma_0$  could be the energy-energy correlation function.

It is also convenient to remove a factor of  $(\alpha_s/\pi)^2$  from the quantity that we calculate. Thus, we calculate

$$\mathcal{I} = \frac{\sigma}{\sigma_0 (\alpha_s/\pi)^2} \quad (2)$$

We note that  $\mathcal{I}$  is a function of the c.m. energy  $\sqrt{s}$ . It is also a function of the  $\overline{\text{MS}}$  renormalization scale  $\mu$ . We will choose  $\mu$  to be proportional to  $\sqrt{s}$ :  $\mu = A_{UV}\sqrt{s}$ . Then  $\mathcal{I}$  depends on  $A$ . But, because it is dimensionless, it is independent of  $\sqrt{s}$ . This allows us to write

$$\mathcal{I} = \int_0^\infty d\sqrt{s} h(\sqrt{s}) \mathcal{I}(A_{UV}, \sqrt{s}) \quad (3)$$

where  $h$  is any function with

$$\int_0^\infty d\sqrt{s} h(\sqrt{s}) = 1. \quad (4)$$

We insert such an integration in the algorithm. Then the integration over  $\sqrt{s}$  eliminates the energy conserving delta function

$$\delta(|\vec{k}_1| + |\vec{k}_2| + |\vec{k}_3| - \sqrt{s}) \quad \text{or} \quad \delta(|\vec{k}_1| + |\vec{k}_2| + |\vec{k}_3| + |\vec{k}_4| - \sqrt{s}) \quad (5)$$

in Eq. (1). This is important in allowing the cancellations of infrared divergences between contributions 3- and 4-particle intermediate state to take place.

## 1.1 What do the signs portend?

We calculate in QCD with  $n_f$  flavors of massless quarks, each coupled with charge  $Q_j e$  to a virtual photon.

We use the Feynman rules as follows, associating factors with either an overall normalization factor  $\mathcal{N}$  or a factor  $\mathcal{G}$  associated with the particular graph.

*Electromagnetic vertices.* For the electromagnetic vertex to the left of the final state cut, the factor  $-iQ_j e$  is associated with  $\mathcal{N}$ . The remaining factor  $\gamma^\mu$  is associated with  $\mathcal{G}$ . For the vertex to the right of the cut, the factor  $+iQ_j e$  is associated with  $\mathcal{N}$ . The remaining factor  $\gamma^\nu$  is associated with  $\mathcal{G}$ . It is convenient to multiply by  $-g_{\mu\nu}$  and sum, including the  $-g_{\mu\nu}$  in  $\mathcal{G}$ . This gives a certain constant  $c_0$  times the observable  $\sigma$ , and we can cancel the constant by calculating  $c_0 \sigma_0$  with this same convention:

$$c_0 \sigma_0 = \left( \sum_j Q_j^2 \right) \frac{N_c s e^2}{2\pi}, \quad (6)$$

where  $N_c$  is the number of colors. (Normally,  $N_c = 3$ , but it is useful to keep  $N_c$  arbitrary in order to make it possible to extract the coefficients of different color factors from the numerical results of the program.)

*QCD vertices.* For each vertex to the left of the cut, we associate a factor  $-ig$  with  $\mathcal{N}$ . For each vertex to the right of the cut, we associate a factor  $+ig$  with  $\mathcal{N}$ . The rest of each vertex factor is associated with  $\mathcal{G}$ .

*Propagators.* For each propagator to the left of the cut, we associate a factor of  $i$  with  $\mathcal{N}$ . For each propagator to the right of the cut, we associate a factor of  $-i$  with  $\mathcal{N}$ . The rest of each propagator factor is associated with  $\mathcal{G}$ . For a cut propagator, there the Feynman rules include a factor  $2\pi\delta(k^2)$ , which we associate entirely with  $\mathcal{G}$ .

*Integrations over loop three-momenta.* The Feynman rules tell us to supply an integration

$$\int \frac{d\vec{l}_j}{(2\pi)^3} \quad (7)$$

for each loop. We associate the factor  $1/(2\pi)^3$  with  $\mathcal{N}$ , the integration  $\int d\vec{l}_j$  with  $\mathcal{G}$ .

*Integrations over loop energies.* The Feynman rules tell us to supply an integration

$$\int \frac{dl_j^0}{2\pi} \quad (8)$$

for each loop. We associate this factor entirely with  $\mathcal{G}$ . (We will see in the next section how we treat the energy integrations.)

*Integration over  $\sqrt{s}$ .* We have, rather artificially, introduced an integration

$$\int_0^\infty d\sqrt{s} h(\sqrt{s}) \quad (9)$$

into the calculation. We associate a factor  $2\pi h(\sqrt{s})$  with  $\mathcal{N}$  and an integration  $\int d\sqrt{s}/(2\pi)$  with  $\mathcal{G}$ . (The integration will be eliminated against a  $2\pi\delta(\sqrt{s} - \sum p_i^0)$ .)

*Virtual loops.* If there is a virtual loop to the left of the cut, we introduce a factor  $1 = i \times (-i)$  and associate the  $+i$  with  $\mathcal{G}$  and the  $-i$  with  $\mathcal{N}$ . (The  $i$  in  $\mathcal{G}$  will cancel a  $-i$  arising from the integration over the loop energy.) If there is a virtual loop to the right of the cut, we associate the  $-i$  with  $\mathcal{G}$  and the  $+i$  with  $\mathcal{N}$ .

*Other factors.* We associate the normalization factor  $1/(c_0\sigma_0(\alpha_s/\pi)^2)$  with  $\mathcal{N}$ .

Collecting the factors to be included in  $\mathcal{N}$ , we have

$$\mathcal{N} = \frac{h(\sqrt{s})}{N_c(2\pi)^3 s} \quad (10)$$

(More generally, this is  $h(\sqrt{s})/[3(2\pi)^{(n+1)}s]$  for a calculation at order  $\alpha_s^n$ .)

## 1.2 Performing the energy integrals

Given a cut  $C$  of a graph  $G$  we replace each cut propagator with label  $P$  by with

$$(2\pi) \theta(\epsilon_P k_P^0) \delta(k_P^\mu k_{P\mu}) \quad (11)$$

where  $k_P^\mu$  is the momentum of the propagator and  $\epsilon_P$  is  $+1$  if the momentum flows across the cut in the positive sense,  $-1$  if it flows across the cut in the negative sense. We integrate over  $k_P^0$ , giving

$$\int \frac{dk_P^0}{2\pi} (2\pi) \theta(\epsilon_P k_P^0) \delta(k_P^\mu k_{P\mu}) = \frac{1}{2|\vec{k}_P|} \quad (12)$$

with  $\epsilon_P k_P^0 = |\vec{k}|$ .

There can be virtual loops. We deal with the case of at most one virtual loop. Consider the case that there is a virtual loop to the left of the cut. Then the integral over the loop energy has the form

$$i \int \frac{dl^0}{2\pi} \frac{1}{(l - Q_1)^2 + i\epsilon} \cdots \frac{1}{(l - Q_n)^2 + i\epsilon} = \\ i \int \frac{dl^0}{2\pi} \prod_n \frac{1}{(l^0 - Q_n^0 - |\vec{l} - \vec{Q}_n| + i\epsilon)(l^0 - Q_n^0 + |\vec{l} - \vec{Q}_n| - i\epsilon)}. \quad (13)$$

We perform the  $l^0$  integration by closing the contour in the lower half plane. This generates a series of terms, one for each propagator in the loop. In a typical term, we replace

$$i \int \frac{dl^0}{2\pi} \frac{1}{(l^0 - Q_J^0 - |\vec{l} - \vec{Q}_J| + i\epsilon)(l^0 - Q_J^0 + |\vec{l} - \vec{Q}_J| - i\epsilon)} \rightarrow \frac{1}{2|\vec{l} - \vec{Q}_J|}. \quad (14)$$

with  $l^0 \rightarrow Q_J^0 + |\vec{l} - \vec{Q}_J|$  in the rest of the integrand. Thus each term corresponds to “cutting” one of the lines in the loop. There is a direction associated with the cut, the direction that we initially chose for the loop momentum  $l$ . Then in the notation used for the ordinary cut propagators, our prescription is to eliminate the energy integration and replace the propagator by

$$\frac{1}{2|\vec{k}_P|} \quad (15)$$

with  $\epsilon_P k_P^0 = |\vec{k}_P|$ , with  $\epsilon_P = +1$  if the momentum  $k_P$  flows in the direction of the cut.

We assign each of the loop propagators in turn to be the cut propagator and make the corresponding replacement.

The rule for virtual loops on the right of the main cut is the same. The propagators come with a  $-i$  and a  $-i\epsilon$ , and we close the contour in the upper half plane, giving the same result

$$\frac{1}{2|\vec{k}_P|}. \quad (16)$$

We can now generalize the concept of a cut. If, after making a cut in the ordinary sense, there is a virtual loop, then we extend the idea of the cut to include the “loop cut” as just described.

### 1.3 The integration over vector loop momenta

The contribution of each cut  $C$  of a graph  $G$  to  $\mathcal{I}$  has the form

$$\mathcal{I}(G, C) = \int dl g(G, C; l). \quad (17)$$

where  $g$  includes  $\int_0^\infty d\sqrt{s} h(\sqrt{s}) \cdots$ . Here  $l = (\vec{l}_1, \vec{l}_2, \vec{l}_3)$  denotes the three loop-momenta:

$$\int dl (\cdots) = \int d\vec{l}_1 d\vec{l}_2 d\vec{l}_3 (\cdots). \quad (18)$$

Thus the cross section is written as a sum

$$\mathcal{I} = \int dl \sum_G \sum_C g(G, C; l). \quad (19)$$

Infrared infinities will cancel between different cuts  $C$  of the same graph  $G$ .

We shall perform the  $l$ -integral numerically by the Monte Carlo method. The loop momenta are chosen as functions a nine-dimensional vector  $X = (x_1, x_2, \dots, x_9)$  in a unit hypercube  $0 < x_i < 1$ . We denote integration over the hypercube as

$$\int dX (\dots) \equiv \int_0^1 dx_1 \int_0^1 dx_2 \cdots \int_0^1 dx_9 (\dots). \quad (20)$$

In the simplest formulation, we would choose the loop momenta  $l$  as a function  $l = M(X)$  of the  $x$ -variables. Then

$$\int dl f(l) = \int dX \frac{f(M(X))}{\rho(M(X))}, \quad (21)$$

where

$$\frac{1}{\rho(M(X))} = \det\left(\frac{\partial M(X)}{\partial X}\right). \quad (22)$$

What we really need to do is a bit more complicated. We have several maps  $M_N$  from  $X$  to  $l$ . Then

$$\int dl f(l) = \int dX \sum_N \frac{f(M_N(X))}{\rho(M_N(X))}. \quad (23)$$

Here

$$\rho(l) = \sum_N \rho_N(l), \quad (24)$$

where

$$\frac{1}{\rho_N(M_N(X))} = \det\left(\frac{\partial M_N(X)}{\partial X}\right). \quad (25)$$

*Proof:* Denoting the inverse of  $l = M_N(X)$  as  $X = M_N^{-1}(l)$  we have

$$\begin{aligned} \sum_N \int dX \frac{f(M_N(X))}{\rho(M_N(X))} &= \sum_N \int dl \det\left(\frac{\partial M_N^{-1}(l)}{\partial l}\right) \frac{f(l)}{\rho(l)} \\ &= \sum_N \int dl \rho_N(l) \frac{f(l)}{\sum \rho_N(l)} \\ &= \int dl f(l). \end{aligned} \quad (26)$$

Thus the cross section is written as

$$\mathcal{I} = \int dX \sum_G \sum_N \sum_C \frac{g(G, C; M_N(X))}{\rho(M_N(X))}. \quad (27)$$

## 1.4 Implementation of the integration

The integration over  $X$  is implemented in the standard Monte Carlo style as a sum over points  $X$  chosen at random:

$$\int dX f(X) \approx \frac{1}{N_{tot}} \sum_{i=1}^{N_{tot}} f(X_i), \quad (28)$$

where the  $X_i$  are chosen at random with density 1 in the unit hypercube. The sum is implemented as a sum over points within a group, then a sum over groups of points:

$$\int dX f(X) \approx \frac{1}{N_R} \sum_{I=1}^{N_R} \Re \bar{f}_I, \quad (29)$$

where

$$\bar{f}_I = \frac{1}{N_G} \sum_{i=1}^{N_G} f(X_{I,i}). \quad (30)$$

The function  $f(X)$  is complex (although the exact integral is real). Thus the integral is approximated by its real part ( $\Re$ ). The corresponding sum of the imaginary parts,  $\Im \bar{f}_I$ , should be approximately zero. We use the error estimate

$$\delta \int dX f(X) \approx \mathcal{E}, \quad (31)$$

where

$$\mathcal{E}^2 = \frac{1}{N_R - 1} \left[ \frac{1}{N_R} \sum_{I=1}^{N_R} (\Re \bar{f}_I)^2 - \left( \frac{1}{N_R} \sum_{I=1}^{N_R} \Re \bar{f}_I \right)^2 \right]. \quad (32)$$

There is a similar error estimate for the imaginary part of the integral.

## 2 The supergraphs

We are concerned with calculating QCD Feynman graphs that are obtained in a simple fashion from cut diagrams that contribute to the discontinuity of the Z-boson self energy, *i.e.* the Fourier transform of  $\langle 0 | T\{J^\mu(x_1)J^\nu(x_2)\} | 0 \rangle$ .

We begin with graphs for the one-particle-irreducible two point function in  $\phi^3$ -theory. We call such a graph a “supergraph.” To each supergraph, we associate several QCD Feynman graphs by letting the propagators represent quark, gluon *etc.* lines. At higher orders of perturbation than that presently considered, four-gluon vertices would appear. The four-gluon interaction would need special treatment. We consider a four-gluon vertex to be the sum of three subgraphs containing two three particle vertices connected by a special propagator – a color-octet spin-two pseudogluon. Then there is a gluon-gluon-pseudogluon vertex in the Feynman rules. Thus we let the  $\phi^3$  propagators represent quark, antiquark,

gluon, ghost, antighost and pseudogluon lines. Each of the resulting Feynman graphs has the same denominator structure.

Our supergraphs must be connected and one-particle irreducible. In addition, propagators that connect a vertex to that same vertex are not allowed. (This does, however, allow one gluon propagator to connect a four-gluon vertex to itself: it connects two different gluon-gluon-pseudogluon vertices.)

For  $N$ -loop graphs, there are  $2N$  vertices, which we label with an index  $V$ . By convention, we take vertex 1 to be the vertex corresponding to  $J^\mu(x_1)$  above, and we take vertex 2 to be the vertex corresponding to  $J^\nu(x_2)$ . We can specify a graph by giving a function  $C$  such that  $C(V, i)$  denotes the index of the  $i$ th vertex connected to vertex  $V$ . Here  $i = 1, 2, 3$ . For the current vertices, 1 and 2, we need a special notation. We consider that the current vertex 1 is connected by the vector boson to the conjugate current vertex, which has label 2. Then  $C(1, 1) = 2$  and  $C(2, 1) = 1$ .

The freedom to relabel the indices  $i$  is used to make

$$C(V, 1) \leq C(V, 2) \leq C(V, 3). \quad (33)$$

The freedom to relabel the vertices  $3, 4, \dots, 2N$  is used to choose a standard labeling. Let  $C$  be a function specifying a certain graph and obeying condition (33). Let  $\pi$  be a permutation of the  $2N - 2$  indices  $3, 4, \dots, 2N$ . Let  $C_\pi$  be the function specifying the graph with vertices relabeled according to  $V \rightarrow \pi(V)$ . To construct  $C_\pi$ , we first define  $C'$  by  $C'(\pi(V), i) = \pi(C(V, i))$ , then construct  $C_\pi$  from  $C'$  by permuting the indices  $i$  for each vertex  $V$  so that  $C_\pi$  obeys condition (33). Evidently, the functions  $C$  and  $C_\pi$  specify the same graph.

Now we can order  $C$  and  $C_\pi$  by defining  $C \prec C_\pi$  if the following conditions hold. First,  $C$  and  $C_\pi$  obey condition (33). Second, there is some  $V_0$  and  $i_0$  such that

$$C(V, i) = C_\pi(V, i) \quad (34)$$

for  $V < V_0$ ,  $i = 1, 2, 3$  and for  $V = V_0$ ,  $i < i_0$  but

$$C(V_0, i_0) < C_\pi(V_0, i_0). \quad (35)$$

The standard labeling is the one for which  $C \prec C_\pi$  or  $C = C_\pi$  for all permutations  $\pi$ . (Notice that  $C = C_\pi$  is possible. Part of the computation of the “counting factor” for  $\phi^3$ -graphs consists of finding how many permutations  $\pi$  leave  $C = C_\pi$ .)

There are  $3N - 1$  propagators, which we label with an index  $P$ . A supergraph may be specified by giving a function  $\mathcal{G}(P, i)$  defined for  $P = 1, \dots, 3N + 1$  and  $i = 1, 2$ . The definition is that  $\mathcal{G}(P, 1)$  is the index of the vertex at the beginning (“tail”) of propagator  $P$ , while  $\mathcal{G}(P, 2)$  is the index of the vertex at the end (“head”) of propagator  $P$ . We also use the index  $P = 0$  to denote the vector boson propagator, with  $G(0, 1) = 2$  and  $G(0, 2) = 1$ . Use of the function  $G$  associates a direction to each propagator, which we define conventionally by the condition that  $G(P, 1) < G(P, 2)$  for  $P = 1, \dots, 3N + 1$ , with, unfortunately, the opposite convention for  $P = 0$ .

There is a freedom to relabel the propagators other than the vector-boson propagator for a given supergraph. We adopt the standard labeling such that  $P_1 < P_2$  implies  $G(P_1, 1) < G(P_2, 1)$ , or  $G(P_1, 1) = G(P_2, 1)$ ,  $G(P_1, 2) \leq G(P_2, 2)$ . (Note that a one loop self-energy subgraph has two propagators with standard labels  $P_1$  and  $P_2 = P_1 + 1$ , with  $G(P_1, i) = G(P_2, i)$ . In this case, permuting the ordering does not affect the function  $G$ .)

The loop momenta are  $\vec{l}_L$ ,  $L = 1, \dots, N$ . We also count the incoming boson momentum  $\vec{Q}$  as one of the loop momenta, namely  $\vec{l}_0$ . We have

$$l_0^0 = \sqrt{s}, \quad \vec{l}_0 = \vec{0}. \quad (36)$$

There are  $3N - 1$  propagators. The propagator momenta are  $\vec{k}_P$ ,  $P = 1, \dots, 3N - 1$ . They are related to the loop momenta  $\vec{l}_L$ ,  $L = 1, \dots, N$  by a matrix  $A$ :

$$\vec{k}_P = \sum_{L=1}^N A_L^P \vec{l}_L, \quad P = 1, \dots, 3N - 1 \quad (37)$$

Extending this to  $P = 0$  and  $L = 0$ , we have

$$k_P^\mu = \sum_{L=0}^N A_L^P l_L^\mu, \quad P = 0, \dots, 3N - 1 \quad \mu = 0, \dots, 3. \quad (38)$$

There are many different possible choices for the loop momenta. We will choose  $\vec{l}_0 = \vec{k}_{Q(0)}$ ,  $\vec{l}_1 = \vec{k}_{Q(1)}, \dots, \vec{l}_N = \vec{k}_{Q(N)}$  for a certain  $(N+1)$ -tuple of indices  $Q(0), Q(1), \dots, Q(N)$ . Evidently, the vectors  $\vec{k}_{Q(L)}$  must be independent in the sense that one can choose them independently without violating momentum conservation. In different parts of the calculation, it is useful to pick different index sets  $\{Q(i)\}$ , and thus different sets of independent loop momenta.

### 3 Review of the numerical method

At this point, we outline the method as a whole before turning to a detailed discussion of the method for sampling points in the space of loop momenta in the immediately following sections.

Let us begin with a precise statement of the problem. We consider an infrared safe three-jet-like observable in  $e^+e^- \rightarrow \text{hadrons}$  such as a particular moment of the thrust distribution. The observable can be expanded in powers of  $\alpha_s/\pi$ ,

$$\sigma = \sum_n \sigma^{[n]}, \quad \sigma^{[n]} \propto (\alpha_s/\pi)^n. \quad (39)$$

The order  $\alpha_s^2$  contribution has the form

$$\sigma^{[2]} = \frac{1}{2!} \int d\vec{p}_1 d\vec{p}_2 \frac{d\sigma_2^{[2]}}{d\vec{p}_1 d\vec{p}_2} \mathcal{S}_2(\vec{p}_1, \vec{p}_2)$$

$$\begin{aligned}
& + \frac{1}{3!} \int d\vec{p}_1 d\vec{p}_2 d\vec{p}_3 \frac{d\sigma_3^{[2]}}{d\vec{p}_1 d\vec{p}_2 d\vec{p}_3} \mathcal{S}_3(\vec{p}_1, \vec{p}_2, \vec{p}_3) \\
& + \frac{1}{4!} \int d\vec{p}_1 d\vec{p}_2 d\vec{p}_3 d\vec{p}_4 \frac{d\sigma_4^{[2]}}{d\vec{p}_1 d\vec{p}_2 d\vec{p}_3 d\vec{p}_4} \mathcal{S}_4(\vec{p}_1, \vec{p}_2, \vec{p}_3, \vec{p}_4).
\end{aligned} \tag{40}$$

Here the  $d\sigma_n^{[2]}$  are the order  $\alpha_s^2$  contributions to the parton level cross section, calculated with zero quark masses. Each contains momentum and energy conserving delta functions. The  $d\sigma_n^{[2]}$  include ultraviolet renormalization in the  $\overline{\text{MS}}$  scheme. The functions  $\mathcal{S}$  describe the measurable quantity to be calculated. We wish to calculate a “three-jet-like” quantity. That is,  $\mathcal{S}_2 = 0$ . The normalization is such that  $\mathcal{S}_n = 1$  for  $n = 2, 3, 4$  would give the order  $\alpha_s^2$  perturbative contribution the total cross section. There are, of course, infrared divergences associated with Eq. (40). For now, we may simply suppose that an infrared cutoff has been supplied.

The measurement, as specified by the functions  $\mathcal{S}_n$ , is to be infrared safe, as described in Ref. [7]: the  $\mathcal{S}_n$  are smooth functions of the parton momenta and

$$\mathcal{S}_{n+1}(\vec{p}_1, \dots, \lambda \vec{p}_n, (1-\lambda) \vec{p}_n) = \mathcal{S}_n(\vec{p}_1, \dots, \vec{p}_n) \tag{41}$$

for  $0 \leq \lambda < 1$ . That is, collinear splittings and soft particles do not affect the measurement.

It is convenient to calculate a quantity that is dimensionless. Let the functions  $\mathcal{S}_n$  be dimensionless and eliminate the remaining dimensionality in the problem by dividing by  $\sigma_0$ , the total  $e^+e^-$  cross section at the Born level. Let us also remove the factor of  $(\alpha_s/\pi)^2$ . Thus, we calculate

$$\mathcal{I} = \frac{\sigma^{[2]}}{\sigma_0 (\alpha_s/\pi)^2}. \tag{42}$$

Let us now see how to set up the calculation of  $\mathcal{I}$  in a convenient form. We note that  $\mathcal{I}$  is a function of the c.m. energy  $\sqrt{s}$  and the  $\overline{\text{MS}}$  renormalization scale  $\mu$ . We will choose  $\mu$  to be proportional to  $\sqrt{s}$ :  $\mu = A_{UV}\sqrt{s}$ . Then  $\mathcal{I}$  depends on  $A$ . But, because it is dimensionless, it is independent of  $\sqrt{s}$ . This allows us to write

$$\mathcal{I} = \int_0^\infty d\sqrt{s} h(\sqrt{s}) \mathcal{I}(A_{UV}, \sqrt{s}), \tag{43}$$

where  $h$  is any function with

$$\int_0^\infty d\sqrt{s} h(\sqrt{s}) = 1. \tag{44}$$

The quantity  $\mathcal{I}$  can be expressed in terms of cut Feynman diagrams, as in Fig. 1. The dots where the parton lines cross the cut represent the function  $\mathcal{S}_n(\vec{p}_1, \dots, \vec{p}_n)$ . Each diagram is a three loop diagram, so we have integrations over loop momenta  $l_1^\mu$ ,  $l_2^\mu$  and  $l_3^\mu$ . We first perform the energy integrations. For the graphs in which four parton lines cross the cut, there are four mass-shell delta functions  $\delta(k_j^2)$ . These delta functions eliminate the three energy integrals over  $l_1^0$ ,  $l_2^0$ , and  $l_3^0$  as well as the integral (44) over  $\sqrt{s}$ . For the graphs in which three parton lines cross the cut, we can eliminate the integration over  $\sqrt{s}$  and two of

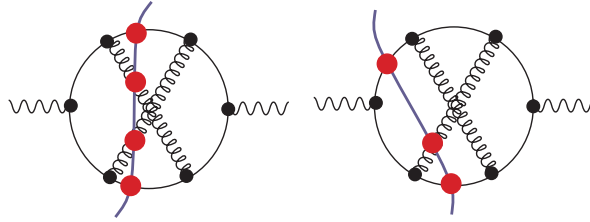


Figure 1: Two cuts of one of the Feynman diagrams that contribute to  $e^+e^- \rightarrow \text{hadrons}$ .

the  $l_J^0$  integrals. One integral over the energy  $E$  in the virtual loop remains. We perform this integration by closing the integration contour in the lower half  $E$  plane. This gives a sum of terms obtained from the original integrand by some simple algebraic substitutions. Having performed the energy integrations, we are left with an integral of the form

$$\mathcal{I} = \sum_G \int d\vec{l}_1 d\vec{l}_2 d\vec{l}_3 \sum_C g(G, C; \vec{l}_1, \vec{l}_2, \vec{l}_3). \quad (45)$$

Here there is a sum over graphs  $G$  (of which one is shown in Fig. 1) and there is a sum over the possible cuts  $C$  of a given graph. The problem of calculating  $\mathcal{I}$  is now set up in a convenient form for calculation.

If we were using the Ellis-Ross-Terrano method, we would put the sum over cuts outside of the integrals in Eq. (45). For those cuts  $C$  that have three partons in the final state, there is a virtual loop. We can arrange that one of the loop momenta, say  $\vec{l}_1$ , goes around this virtual loop. The essence of the ERT method is to perform the integration over the virtual loop momentum analytically ahead of time. The integration is often ultraviolet divergent, but the ultraviolet divergence is easily removed by a renormalization subtraction. The integration is also typically infrared divergent. This divergence is regulated by working in  $3 - 2\epsilon$  space dimensions and then taking  $\epsilon \rightarrow 0$  while dropping the  $1/\epsilon^n$  contributions (after proving that they cancel against other contributions). After the  $\vec{l}_1$  integration has been performed analytically, the integrations over  $\vec{l}_2$  and  $\vec{l}_3$  can be performed numerically. For the cuts  $C$  that have four partons in the final state, there are also infrared divergences. One uses either a “phase space slicing” or a “subtraction” procedure to get rid of these divergences, cancelling the  $1/\epsilon^n$  pieces against the  $1/\epsilon^n$  pieces from the virtual graphs. In the end, we are left with an integral  $\int d\vec{l}_1 d\vec{l}_2 d\vec{l}_3$  in exactly three space dimensions that can be performed numerically.

In the numerical method, we keep the sum over cuts  $C$  inside the integrations. We take care of the ultraviolet divergences by simple renormalization subtractions on the integrand. We make certain deformations on the integration contours so as to keep away from poles of the form  $1/[E_F - E_I \pm i\epsilon]$ , where  $E_F$  is the energy of the final state and  $E_I$  is the energy of an intermediate state. Then the integrals are all convergent and we calculate them by Monte Carlo numerical integration.

Let us now look at the contour deformation in a little more detail. We denote the momenta  $\{\vec{l}_1, \vec{l}_2, \vec{l}_3\}$  collectively by  $l$  whenever we do not need a more detailed description.

Thus

$$\mathcal{I} = \sum_G \int dl \sum_C g(G, C; l). \quad (46)$$

For cuts  $C$  that leave a virtual loop integration, there are singularities in the integrand of the form  $E_F - E_I + i\epsilon$  (or  $E_F - E_I - i\epsilon$  if the loop is in the complex conjugate amplitude to the right of the cut). Here  $E_F$  is the energy of the final state defined by the cut  $C$  and  $E_I$  is the energy of a possible intermediate state. We will examine the nature of these “scattering singularities” in some detail in the next section. For now, all we need to know is that  $E_F - E_I = 0$  on a surface in the space of  $\vec{l}_1$  for fixed  $\vec{l}_2$  and  $\vec{l}_3$  if we pick  $\vec{l}_1$  to be the momentum that flows around the virtual loop. These singularities do not create divergences. The Feynman rules provide us with the  $i\epsilon$  prescriptions that tell us what to do about the singularities: we should deform the integration contour into the complex  $\vec{l}_1$  space so as to keep away from them. Thus we write our integral in the form

$$\mathcal{I} = \sum_G \int dl \sum_C \mathcal{J}(G, C; l) g(G, C; l + i\kappa(G, C; l)). \quad (47)$$

Here  $i\kappa$  is a purely imaginary nine-dimensional vector that we add to the real nine-dimensional vector  $l$  to make a complex nine-dimensional vector. The imaginary part  $\kappa$  depends on the real part  $l$ , so that when we integrate over  $l$ , the complex vector  $l + i\kappa$  lies on a surface, the integration contour, that is moved away from the real subspace. When we thus deform the contour, we supply a jacobian  $\mathcal{J} = \det(\partial(l + i\kappa)/\partial l)$ . (See Ref. [4] for details.)

The amount of deformation  $\kappa$  depends on the graph  $G$  and, more significantly, the cut  $C$ . For cuts  $C$  that leave no virtual loop, each of the momenta  $\vec{l}_1$ ,  $\vec{l}_2$ , and  $\vec{l}_3$  flows through the final state. For practical reasons, we want the final state momenta to be real. Thus we set  $\kappa = 0$  for cuts  $C$  that leave no virtual loop. On the other hand, when the cut  $C$  does leave a virtual loop, we choose a non-zero  $\kappa$ . We must, however, be careful. When  $\kappa = 0$  there are singularities in  $g$  on certain surfaces that correspond to collinear parton momenta. These singularities cancel between  $g$  for one cut  $C$  and  $g$  for another. This cancellation would be destroyed if, for  $l$  approaching the collinear singularity,  $\kappa = 0$  for one of these cuts but not for the other. For this reason, we insist that for all cuts  $C$ ,  $\kappa \rightarrow 0$  as  $l$  approaches one of the collinear singularities. The details can be found in Ref. [4]. All that is important here is that  $\kappa \rightarrow 0$  quadratically with the distance to a collinear singularity.

Much has been left out in this brief overview, but we should now have enough background to see the requirements for a sensible choice of integration points.

## 4 General principles for the choice of points

In the following sections, we discuss the choice of integration points for the evaluation of a given graph. In this section, we summarize the general principles of Monte Carlo integration as they apply to this calculation.

We wish to perform an integral of the form

$$\mathcal{I} = \sum_G \int dl f(G; l) \quad (48)$$

where

$$f(G; l) = \Re \left\{ \sum_C \mathcal{J}(G, C; l) g(G, C; l + i\kappa(G, C; l)) \right\}. \quad (49)$$

(We can take the real part because we know in advance that  $\mathcal{I}$  is real.) Using the Monte Carlo technique, for each graph  $G$  we choose a large number  $\xi(G)N$  of points  $l$ , with  $\sum_G \xi(G) = 1$  so that the total number of points is  $N$ . We sample the points  $l$  for graph  $G$  at random with a density  $\rho(G; l)$ , with normalization  $\int dl \rho(G; l) = 1$ . Then the integral is approximated by

$$\mathcal{I}_N = \frac{1}{N} \sum_G \frac{1}{\xi(G)} \sum_{j=1}^{\xi(G)N} \frac{f(l_j)}{\rho(G; l_j)}. \quad (50)$$

This is an approximation for the integral in the sense that, if we repeat the procedure a lot of times, the expectation value for  $\mathcal{I}_N$  is

$$\langle \mathcal{I}_N \rangle = \mathcal{I}. \quad (51)$$

The expected r.m.s. error is  $\mathcal{E}$ , where

$$\mathcal{E}^2 = \langle (\mathcal{I}_N - \mathcal{I})^2 \rangle. \quad (52)$$

With a little manipulation, one can rewrite this as

$$\mathcal{E}^2 = \frac{1}{N} \left\{ \sum_G \xi(G) \left[ \frac{\Delta(G)}{\xi(G)} - \sum_L \Delta(L) \right]^2 + \left( \sum_L \Delta(L) \right)^2 \right\}. \quad (53)$$

where

$$\begin{aligned} \Delta(G)^2 &= \int dl \rho(G; l) \left[ \frac{|f(G; l)|}{\rho(G; l)} - \int dl' |f(G; l')| \right]^2 \\ &\quad + \int dl (|f(G; l)| + f(G; l)) \times \int dl' (|f(G; l')| - f(G; l')). \end{aligned} \quad (54)$$

We see, first of all, that the expected error decreases proportionally to  $1/\sqrt{N}$ . Second, we see that for a given choice of the density functions  $\rho(G; l)$ , the ideal choice of the factors  $\xi(G)$  is  $\xi(G) \propto \Delta(G)$ . This is, in fact, easy to implement. Third, the ideal choice of  $\rho(G; l)$  is  $\rho(G; l) \propto |f(G; l)|$ . This is, in fact, impossible to implement.

Although it is not possible to choose  $\rho(G; l) \propto |f(G; l)|$ , at least we can choose it so that  $|f(G; l)|/\rho(G; l)$  is not singular at the singularities of  $|f(l)|$ . Furthermore, we can try to make  $\rho(G; l)$  big at places where we know that  $|f(G; l)|$  is big.

We will build the general sampling method out of elementary sampling methods. That is, we will find a number of simple methods to choose points  $l$  for our graph. Let the density of points for the  $i$ th elementary sampling method be  $\rho_i(G; l)$  (normalized to  $\int dl \rho_i(G; l) = 1$ ). Then we devote a fraction  $\lambda_i(G)$  of the points to the choice with density  $\rho_i(G; l)$  and obtain a net density

$$\rho(G; l) = \sum_i \lambda_i(G) \rho_i(G; l). \quad (55)$$

In this way, we make the sampling problem manageable. If we know that  $|f(G; l)|$  is big near a certain point or surface in the space of loop momenta, we can design one of the elementary sampling methods so that the corresponding  $\rho_i(G; l)$  is big there. In undertaking this task, we do not have to simultaneously arrange that  $\rho_i(G; l)$  be big at other places where  $|f(G; l)|$  is big.

In the following sections, we discuss the elementary sampling methods. We imagine that we are dealing with only one specific graph  $G$ , so we suppress the index  $G$  in the notation.

## 5 Organization of the sampling method

We consider a fixed (uncut) graph, dropping references to the label  $G$  of the graph. As mentioned in the previous section, we sample points  $l$  in the space of loop momenta according to several elementary sampling methods, each labelled by an index  $i$  and having a density of points  $\rho_i(l)$ . The net density is then  $\rho(l) = \sum \lambda_i \rho_i(l)$ .

We first address the identification of loop momenta. There are eight propagator momenta  $\vec{k}_P$ . (See, for example, Fig. 1.) The three loop momenta  $\vec{l}_L$  can in general be any three linearly independent linear combinations of the  $\vec{k}_P$ . We will keep the choice simple by choosing three of the  $\vec{k}_P$  to be the loop momenta. However, this still leaves us with the choice of which three of the  $\vec{k}_P$  should be loop momenta. It proves convenient to make *different* choices for different elementary sampling methods. We specify the choice by specifying a triplet of integers  $\{Q(1), Q(2), Q(3)\}$  such that  $\vec{l}_J$  is  $\vec{k}_{Q(J)}$ . We call  $Q$  an index set. Then the complete set of propagator matrices can be related to the loop momenta by a matrix  $A$ :

$$\vec{k}_P = \sum_{L=1}^3 A_L^P \vec{l}_L. \quad (56)$$

Evidently, given the index set  $Q$ , the matrix  $A$  can be constructed by using the topology of the graph.

Now we characterize certain surfaces, to be called scattering singularity surfaces, near which the integrand  $|f(l)|$  is big. To do this, we consider the cuts of our graph in which three partons appear in the final state. For each such cut, there is a virtual loop. Let  $\vec{l}_1$  be the loop momentum. More precisely,  $\vec{l}_1$  will be the momentum,  $\vec{k}_{Q(1)}$ , of one of the propagators in the loop, but we defer for a moment specifying which one. As specified in Sec. 3, the integration contour for  $\vec{l}_1$  is deformed into the complex plane,<sup>1</sup> so that  $\vec{l}_1 \rightarrow \vec{l}_{1,c} = \vec{l}_1 + i\vec{\kappa}$ .

---

<sup>1</sup>We keep the momenta that enter the final state real.

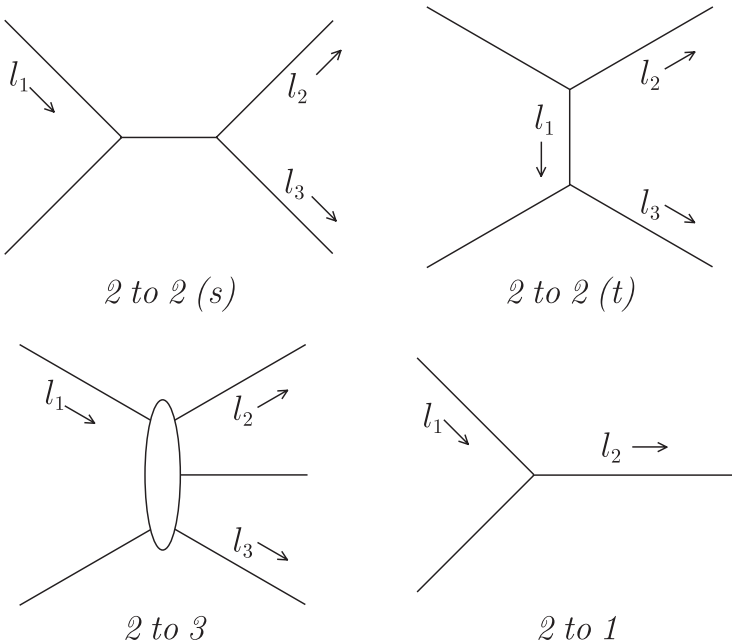


Figure 2: Elementary scattering subdiagrams that occur at next-to-leading order.

Before deformation, the integrand is singular on certain surfaces associated with simple scattering processes, the scattering singularity surfaces. How can this happen? There are four cases. Each case is illustrated by a Feynman graph in Fig. 2. The corresponding scattering singularity surface is illustrated in Fig. 3. The cases are

1. *2 to 2 (s)*. A virtual parton with momentum  $\vec{l}_1$  merges with a virtual parton with momentum  $\vec{l}_2 + \vec{l}_3 - \vec{l}_1$  to produce a virtual parton with momentum  $\vec{l}_2 + \vec{l}_3$ . This virtual parton divides into two partons with momenta  $\vec{l}_2$  and  $\vec{l}_3$  that enter the final state. In old-fashioned perturbation theory, there is an energy denominator  $|\vec{l}_2| + |\vec{l}_3| - |\vec{l}_1| - |\vec{l}_2 + \vec{l}_3 - \vec{l}_1| + i\epsilon$ , which vanishes on the ellipsoid  $|\vec{l}_1| + |\vec{l}_2 + \vec{l}_3 - \vec{l}_1| = |\vec{l}_2| + |\vec{l}_3|$  in the space of  $\vec{l}_1$ . This is the scattering singularity surface. The contour deformation is non-zero on the entire scattering singularity surface.
2. *2 to 2 (t)*. A virtual parton with momentum  $\vec{l}_2 + \vec{l}_1$  scatters from a virtual parton with momentum  $\vec{l}_3 - \vec{l}_1$  by exchanging a parton with momentum  $\vec{l}_1$ . Partons with momentum  $\vec{l}_2$  and  $\vec{l}_3$  emerge into the final state. There is a scattering singularity surface  $|\vec{l}_2 + \vec{l}_1| + |\vec{l}_3 - \vec{l}_1| = |\vec{l}_2| + |\vec{l}_3|$ . In this case, there is also a singularity at  $\vec{l}_1 = 0$  that arises from the propagator of the exchanged parton. This soft exchange singularity lies on the scattering singularity surface. Furthermore, in our treatment, the contour deformation vanishes at the soft exchange singularity so that, even after contour deformation, the integrand is singular there. This is, however, an integrable singularity.

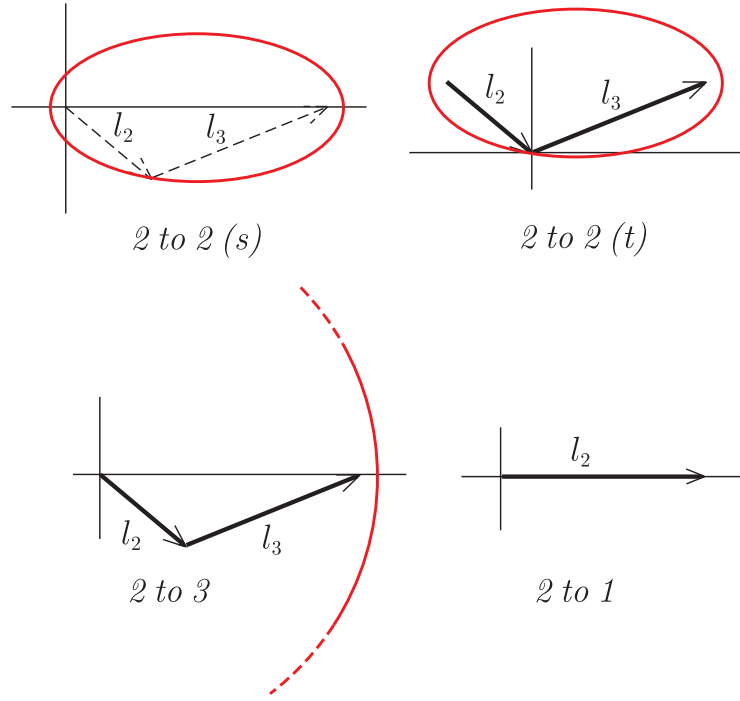


Figure 3: Singularity surfaces associated with the elementary scatterings in Fig. 2. In each case, the vectors  $\vec{l}_2$  and  $\vec{l}_3$  (or just  $\vec{l}_2$  for 2 to 1 scattering) are indicated by arrows. We see the scattering singularity surface in the space of  $\vec{l}_1$ . For 2 to 2 (*t*) scattering and 2 to 2 (*s*) scattering, these surfaces are ellipsoids. For 2 to 3 scattering, the surface is a sphere, only part of which is shown. For 2 to 1 scattering, the surface reduces to a line segment. The integrand is typically not singular on the scattering singularity surface because of the contour deformation. However, the contour deformation vanishes along the heavy straight lines. Thus, in particular, in the 2 to 2 (*t*) case the integrand is actually singular at  $\vec{l}_1 = 0$ .

3. *2 to 3.* A virtual parton with momentum  $\vec{l}_1$  collides with a virtual parton with momentum  $-\vec{l}_1$  to produce a final state with partons carrying momenta  $\vec{l}_2$ ,  $\vec{l}_3$ , and  $-\vec{l}_2 - \vec{l}_3$ . There is an energy denominator  $|\vec{l}_2| + |\vec{l}_3| + |\vec{l}_2 + \vec{l}_3| - 2|\vec{l}_1| + i\epsilon$ , which is singular on the sphere  $|\vec{l}_1| = [|\vec{l}_2| + |\vec{l}_3| + |\vec{l}_2 + \vec{l}_3|]/2$ . The contour deformation is non-zero on the entire scattering singularity surface.
4. *2 to 1.* A virtual parton with momentum  $\vec{l}_1$  combines with a virtual parton with momentum  $\vec{l}_2 - \vec{l}_1$  to produce an on shell parton with momentum  $\vec{l}_2$  that enters the final state. There is an energy denominator  $|\vec{l}_2| - |\vec{l}_1| - |\vec{l}_2 - \vec{l}_1| + i\epsilon$ , which vanishes on the line  $\vec{l}_1 = x\vec{l}_2$  with  $0 \leq x \leq 1$ . The contour deformation is chosen to vanish at this collinear singularity. As discussed in Ref. [4], the collinear singularity cancels when one sums over cuts. However, singularities at  $\vec{l}_1 = 0$  and  $\vec{l}_1 = \vec{l}_2$  remain.

Thus for each cut there are a number of scattering singularity surfaces. There is a contour deformation that keeps the integrand from being singular except at special points on these surfaces. However, the integrand is sometimes still quite large near these surfaces. For this reason, we will design an elementary sampling method for each surface such that the density of points is big on the whole surface and singular at the special point if necessary.

There are two kinds of singularities associated with points  $\vec{k}_P = 0$  where a propagator momentum vanishes. First, there is a  $1/|\vec{k}_P|^2$  singularity when the momentum of the exchanged parton in a *2 to 2 (t)* scattering vanishes. The elementary sampling method associated with the *2 to 2 (t)* scattering will be designed to take care of this kind of singularity. Second, there is a  $1/|\vec{k}_P|$  singularity when *any* propagator momentum  $\vec{k}_P$  approaches zero. This weak singularity arises simply because massless Lorentz invariant phase space is  $d\vec{k}/|\vec{k}|$ . As it turns out, these singularities in the density will automatically be provided by the combined sampling methods without having to specifically arrange for them.

The *2 to 1* scattering singularity surface is exceptional in the list above in that there is no singularity except for the two singular points at  $\vec{l}_1 = 0$  and  $\vec{l}_2 - \vec{l}_1 = 0$ . These two singular points are of one or the other of two types mentioned above. Typically a *2 to 1* scattering subdiagram is part of a *2 to 2 (s)* or *2 to 2 (t)* scattering subdiagram and the two singularities are provided for by the *2 to 2 (s)* or *2 to 2 (t)* sampling methods. The exception is in the case of a self-energy subgraph that is connected to a final state parton. In this case, the *2 to 2 (t)*, *2 to 2 (s)*, and *2 to 3* sampling methods do not apply and we need an explicit *2 to 1* sampling method. Thus we will apply a *2 to 1* sampling method only in the case of a self-energy subgraph connected to a final state parton.

The previous argument indicates that for each scattering singularity surface in the space of the loop momentum  $\vec{l}_1$  in a virtual loop, we should associate a method for choosing  $\vec{l}_1$  that puts a high density of points near this surface. It is then useful to choose the other two loop momenta to be the momenta of two of the three partons in the final state. Thus the momenta of the final state partons are  $\vec{l}_2$ ,  $\vec{l}_3$ , and  $-\vec{l}_2 - \vec{l}_3$ . The integrand will be singular whenever the three partons approach a two jet configuration. Thus we choose the points  $\{\vec{l}_2, \vec{l}_3\}$  so that the density of points is appropriately singular at the two jet configurations.

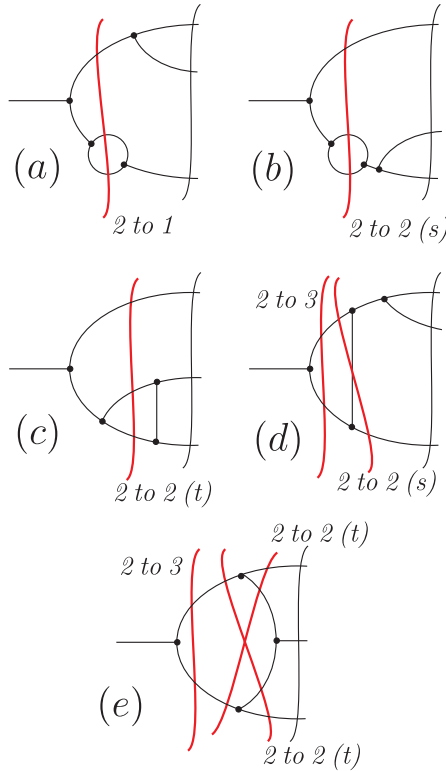


Figure 4: Matching of scattering singularities to the structure of one loop virtual subdiagrams. A scattering singularity occurs when the energy of an intermediate state matches the energy of the final state. For each diagram, the relevant intermediate states are marked with a line through the graph. The label near the line indicates the type of the corresponding singularity. For some graphs, there is more than one scattering singularity, as indicated. The *2 to 1* singularity is marked only in the case of a self-energy subdiagram connected to a final state parton.

Thus we have a general scheme for organizing the elementary sampling methods. First, find all of the possible three parton cuts of the graph in question. Then, for each such final state cut, enumerate the scattering singularity surfaces that can occur, counting the *2 to 1* case only when the virtual loop is a self-energy diagram connected to a final state parton. There are five basic situations, as illustrated in Fig. 4. Each combination of a final state cut and a scattering singularity surface will correspond to an elementary sampling method.

One point should be emphasized for clarity. In the numerical method discussed in this paper, for each integration point, we compute  $f/\rho$  where  $f$  is the integrand and  $\rho$  is the density of integration points. Contributions from all cuts of a given graph are calculated and summed to form the integrand  $f$ . The density  $\rho$  is also a sum, with terms corresponding to each of the possible cuts of the graph. Thus there are *independent* sums over possible cuts in  $f$  and in  $\rho$ .

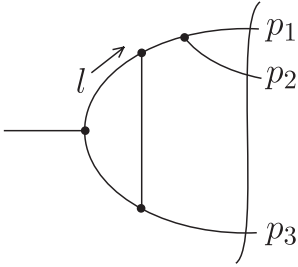


Figure 5: Labelling of momenta for graphs of type (d) in Fig. 4.

Consider the five basic amplitudes with a virtual loop that are illustrated in Fig. 4. In two of these cases, there are more than one possible intermediate state involving the virtual loop and thus more than one scattering singularity surface. In these cases, it is important to understand how the scattering singularity surfaces fit together.

Let us examine, then, case (d) in Fig. 4. Label the momenta as in Fig. 5. In Fig. 6 we see the scattering singularity surfaces in the space of the loop momentum  $\vec{l} \equiv \vec{l}_1$  for an arbitrary fixed choice of the final state momenta  $\vec{p}_j$ . (We draw the figure for  $\vec{l}$  in the plane of the  $\vec{p}_j$ ). The vectors  $\vec{p}_1$ ,  $\vec{p}_2$ , and  $\vec{p}_3$  are indicated. The integration contour is deformed everywhere except along the line  $\vec{l} = -x\vec{p}_3$  with  $0 < x < 1$ , which is indicated as a solid line. There is an ellipsoidal  $2 \text{ to } 2$  (*s*) surface,  $|\vec{l}| + |\vec{p}_1 + \vec{p}_2 - \vec{l}| = |\vec{p}_1| + |\vec{p}_2|$ . There is also a spherical  $3 \text{ to } 2$  surface,  $2|\vec{l}| = |\vec{p}_1| + |\vec{p}_2| + |\vec{p}_3|$ . The integration contour is deformed everywhere on both of these surfaces, so that the integrand is not singular anywhere. On the other hand, the deformation vanishes on the solid line, which can be rather near the ellipsoidal surface in the case that the angle between  $\vec{p}_1$  and  $\vec{p}_2$  is small. Thus the integrand can be rather big on the ellipsoid in this circumstance. Furthermore, the size of the integrand is enhanced where the ellipsoid is tangent to the spherical singularity surface. We will need to put an extra density of points in the region of this point of tangency.

Case (e) in Fig. 4 just a little more complicated. Label the momenta as in Fig. 7. Fig. 6 shows the scattering singularity surfaces in the space of the loop momentum  $\vec{l}$  for fixed final state momenta  $\vec{p}_j$ . The vectors  $\vec{p}_1$ ,  $\vec{p}_2$ , and  $\vec{p}_3$  are indicated. The integration contour is deformed everywhere except along the lines  $\vec{l} = x\vec{p}_1$ ,  $\vec{l} - \vec{p}_1 = x\vec{p}_2$  and  $\vec{l} - \vec{p}_1 - \vec{p}_2 = x\vec{p}_3$ , with  $0 < x < 1$  in each case. These lines are indicated as solid lines that form a triangle. There are two ellipsoidal  $2 \text{ to } 2$  (*t*) surfaces,  $|\vec{l}| + |\vec{p}_1 + \vec{p}_2 - \vec{l}| = |\vec{p}_1| + |\vec{p}_2|$  and  $|\vec{l} - \vec{p}_1| + |\vec{l}| = |\vec{p}_2| + |\vec{p}_3|$ . There is also a spherical  $3 \text{ to } 2$  surface,  $2|\vec{l}| = |\vec{p}_1| + |\vec{p}_2| + |\vec{p}_3|$ . As in the previous case, (d), we need an especially high density of integration points near where an ellipsoid is tangent to the sphere in the case that this point is near to the triangle, where the deformation vanishes. We have also the new feature that each of the ellipsoids shares a point with the triangle. At this point the contour deformation is zero, so the integrand is actually singular. This is the point where the momentum of the exchanged parton in the associated  $2 \text{ to } 2$  (*t*) scattering vanishes. The density of integration points will have to have a corresponding singularity at these points.

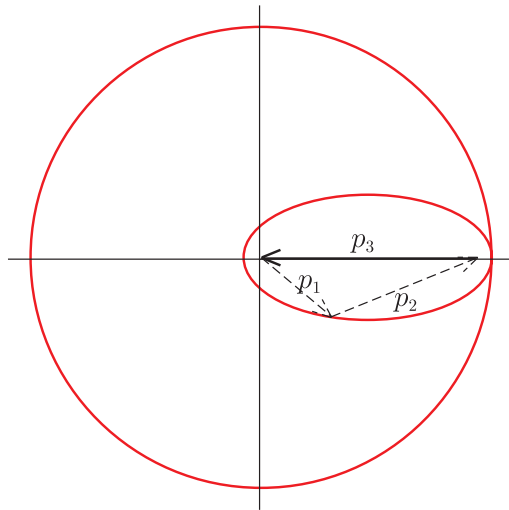


Figure 6: Singularity surfaces for graphs of type (d) in Fig. 4.

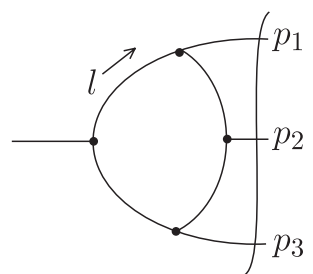


Figure 7: Labelling of momenta for graphs of type (e) in Fig. 4.

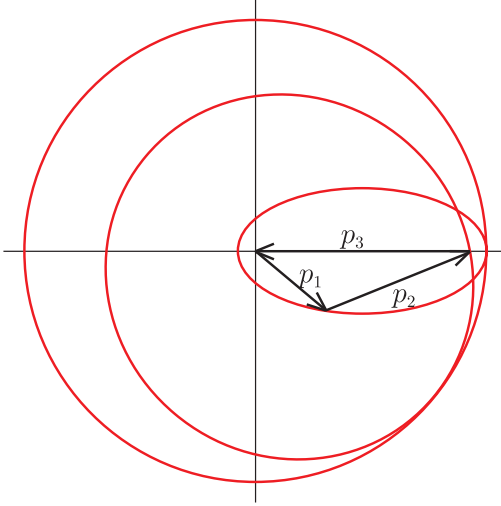


Figure 8: Singularity surfaces for graphs of type (e) in Fig. 4.

This completes the description of the general organization of the sampling scheme. In the following sections, we outline its component parts.

## 6 Sampling for the final state

As discussed in the previous section, for each final state cut with three partons in the final state, we will define a number of elementary sampling methods. Part of each method is to choose with an appropriate density the momentum  $\vec{l}_1$  that circles through the virtual loop that occurs when there are three final state partons. The other part is to choose the momenta  $\vec{l}_2$ ,  $\vec{l}_3$ , and  $-\vec{l}_2 - \vec{l}_3$  of the final state partons. We address the choice of the final state momenta in this section.

Let the final state parton momenta be  $\vec{p}_1$ ,  $\vec{p}_2$ , and  $\vec{p}_3$ , with  $\sum_i \vec{p}_i = 0$ . (Two of these will then be  $\vec{l}_2$  and  $\vec{l}_3$ , but it doesn't matter which ones.) Define  $E_{\max} = \frac{1}{2} \sum_i |\vec{p}_i|$  and  $x_i = |\vec{p}_i|/E_{\max}$ . Then  $\sum_i x_i = 2$  and  $0 \leq x_i \leq 1$ . We can write the integration over final state momenta as follows, using  $p_3^2 = p_1^2 + p_2^2 + 2p_1 p_2 \cos \theta_{12}$  so that  $d \cos \theta_{12} = p_3 dp_3 / (p_1 p_2)$ :

$$\begin{aligned} \mathcal{I} &= \int d\vec{p}_1 d\vec{p}_2 d\vec{p}_3 \delta(\sum \vec{p}_i) f(p) \\ &= \int 2E_{\max}^6 d \ln E_{\max} d \cos \theta_1 d\phi_1 d\phi_{12} x_1 x_2 x_3 dx_1 dx_2 f(p). \end{aligned} \quad (57)$$

Here  $\{\theta_1, \phi_1\}$  are the angles of  $\vec{p}_1$  and  $\phi_{12}$  is the angle between  $\vec{p}_1 \times \vec{p}_2$  and  $\vec{p}_1 \times \vec{e}$ , where  $\vec{e}$  is an arbitrary reference vector.

If we sample  $\{\ln E_{\max}, \cos \theta_1, \phi_1, \phi_{12}\}$  with a density

$$\rho_A \equiv \frac{dN}{d \ln E_{\max} d \cos \theta_1 d\phi_1 d\phi_{12}} \quad (58)$$

and we sample  $\{x_1, x_2\}$  with a density

$$\rho_B \equiv \frac{dN}{dx_1 dx_2}, \quad (59)$$

then the net density is

$$\rho \equiv \frac{dN}{d\vec{p}_1 d\vec{p}_2} = \frac{\rho_A \rho_B}{2E_{\max}^6 x_1 x_2 x_3}. \quad (60)$$

On symmetry grounds,  $\rho_A$  should be independent of the angles. Its dependence on  $E_{\max}$  is not too important. A convenient choice, normalized so that  $\int dN = 1$ , is

$$\frac{1}{\rho_A} = \frac{8\pi^2}{3} (E_0/E_{\max})^3 [1 + (E_{\max}/E_0)^3]^2, \quad (61)$$

where  $E_0$  is a fixed parameter with dimensions of mass.

What should be the properties of  $\rho_B$ ? We can expect the integrand  $f(p)$  to be singular in any two jet region: when any of the  $\vec{p}_j$  vanishes ( $x_j \rightarrow 0$ ) or when two of them become collinear (if  $\vec{p}_1$  and  $\vec{p}_2$  are nearly collinear, then  $x_3 \approx 1$ ). The factor  $1/x_1 x_2 x_3$  in Eq. (60) provides a weak singularity in the  $x_i \rightarrow 0$  regions. We can build in a weak singularity in the collinear regions by choosing

$$\rho_B = \frac{\mathcal{N}_x \max_j \sqrt{1-x_j}}{\prod_j \sqrt{1-x_j}}. \quad (62)$$

The  $x_i \rightarrow 0$  regions are at the intersections of  $x_l \rightarrow 1$  regions, so these collinear singularities also enhance the soft singularity of the density. The normalization constant is fixed so that  $\int dN = 1$  and is  $\mathcal{N}_x = 1/(6\sqrt{2} \arcsin(1/\sqrt{3}))$ . One can, of course, change  $1/\sqrt{1-x}$  to  $1/(1-x)^A$  for any  $A$  smaller than 1.

It is a simple matter to actually choose points with the density  $\rho$  in Eq. (60). Readers interested in the implementation details may consult the notes [6] that accompany the program code.

I can comment here about the singularities of the integrand,  $f$ . If, for the moment, we set the measurement function to 1, then the nominal behavior of  $f$  is  $f \propto 1/x_j^3$  for  $x_j \rightarrow 0$  and  $f \propto 1/(1-x_j)$  for  $x_j \rightarrow 1$ . This nominal behavior is what one gets after performing the virtual loop integral,  $\int dl_1$ , inside the  $\{\vec{p}_1, \vec{p}_2\}$  integral [8]. These singularities make the integration logarithmically divergent. Then the measurement function that is included in  $f$  is required to vanish in the two jet limit, so that the integration becomes convergent. Now, in fact, if we look at the singularities in the  $\{\vec{p}_1, \vec{p}_2\}$  integral before performing the virtual loop integral, the singularities are worse than this nominal behavior. For this reason, the suppression of the two jet region coming from the measurement function must be suitably strong in order to obtain good convergence. It remains for future research to arrange the calculation in such a way that the nominal behavior of the integrand  $f$  as a function of  $\{\vec{p}_1, \vec{p}_2\}$  is obtained.

There are two steps to choosing the points. First, we need to sample the variables  $\{\ln E_{\max}, \cos \theta_1, \phi_1, \phi_{12}\}$  with a density  $\rho_A$  with

$$\frac{1}{\rho_A} = \frac{8\pi^2}{3} (E_0/E_{\max})^3 \left[1 + (E_{\max}/E_0)^3\right]^2, \quad (63)$$

This is accomplished by choosing numbers  $\{X_1, X_2, X_3, X_4\}$  at random in the interval  $0 < X_j < 1$  and then setting

$$\begin{aligned} E_{\max} &= E_0 \left( \frac{1}{X_1} - 1 \right)^{1/3} \\ \cos \theta_1 &= 2X_2 - 1 \\ \phi_1 &= 2\pi X_3 \\ \phi_{12} &= 2\pi X_4. \end{aligned} \quad (64)$$

Next we want to sample the variables  $\{x_1, x_2, x_3\}$  with  $\sum x_j = 2$  in the region  $0 < x_j < 1$  with density

$$\rho_B = \frac{\mathcal{N}_x \max_j \sqrt{1-x_j}}{\prod_j \sqrt{1-x_j}}. \quad (65)$$

where  $\mathcal{N}_x = 1/(6\sqrt{2} \arcsin(1/\sqrt{3}))$ . Taking into account the constraint  $\sum x_j = 2$ , the region in the space  $\{x_1, x_2\}$  is the triangle  $\{x_1 < 1, x_2 < 1, 2 - x_1 - x_2 < 1\}$ .

To implement the sampling, it is *not* convenient to use a single mapping from a unit square to the  $\{x_1, x_2\}$  triangle. Rather, we divide the triangle into three regions according to which of  $x_1, x_2, x_3$  is the smallest. We determine which of the three regions a point is to go into at random, with probability 1/3 for each region. Suppose that the chosen region is  $\mathcal{R}_{12} = \{x_3 < x_1 < 1, x_3 < x_2 < 1\}$ . Stated in terms of  $x_1$  and  $x_2$ , this region is

$$\mathcal{R}_{12} = \{x_1 < 1, x_2 < 1, 1 < x_1 + x_2/2, 1 < x_2 + x_1/2\}. \quad (66)$$

In this region we want to choose points  $\{x_1, x_2\}$  with a density

$$\rho_B = \frac{\mathcal{N}_x}{\sqrt{(1-x_1)(1-x_2)}}. \quad (67)$$

To do this, we choose parameters  $X_a, X_b$  at random in  $0 < X_i < 1$  and put

$$x_1 = 1 - X_a^2/2, \quad x_2 = 1 - X_b^2/2. \quad (68)$$

This gives a density of points proportional to  $1/[(1-x_1)(1-x_2)]^{1/2}$  as required. The points will lie in the square  $\{0 < 1 - x_1 < 1/2, 0 < 1 - x_2 < 1/2\}$ , which contains the region  $\mathcal{R}_{12}$ . If a chosen point is not in  $\mathcal{R}_{12}$ , we simply throw it out and choose a different point.

This gives an overall density  $\rho$  with

$$\rho = \frac{C \max_j \sqrt{1-x_j}}{E_0^3 E_{\max}^3 \left[1 + (E_{\max}/E_0)^3\right]^2 x_1 x_2 x_3 \prod_j \sqrt{1-x_j}} \quad (69)$$

where

$$C = \frac{1}{32\sqrt{2}\pi^2 \arcsin(1/\sqrt{3})} = 0.0036376552621307193655\dots \quad (70)$$


---

## 7 Sampling for 2 to 2 ( $s$ ) scattering

In this section, we consider the sampling method associated with 2 to 2 ( $s$ ) scattering. We need to choose points  $\vec{l} \equiv \vec{l}_1$  appropriate to the following case:

A virtual parton with momentum  $\vec{l}$  merges with a virtual parton with momentum  $\vec{l}_2 + \vec{l}_3 - \vec{l}$  to produce a virtual parton with momentum  $\vec{l}_2 + \vec{l}_3$ . This virtual parton divides into two partons with momenta  $\vec{l}_2$  and  $\vec{l}_3$  that enter the final state.

In this case, the scattering surface is the ellipsoid  $|\vec{l}| + |\vec{l}_2 + \vec{l}_3 - \vec{l}| = |\vec{l}_2| + |\vec{l}_3|$ . The density of points should be large on this surface. In order to accomplish this, we use elliptical coordinates.

### 7.1 Elliptical coordinates

The elliptical coordinates  $A_+, A_-, \phi$  are defined as follows. First, define  $\kappa$  by

$$2\kappa = |\vec{l}_2 + \vec{l}_3|. \quad (71)$$

Now, define coordinates  $A_{\pm}$  by

$$A_{\pm} = \frac{1}{2\kappa} (|\vec{l}| \pm |\vec{l} - \vec{l}_2 - \vec{l}_3|). \quad (72)$$

Then

$$1 < A_+, \quad -1 < A_- < 1. \quad (73)$$

The coordinate  $A_+$  is constant on elliptical surfaces, while  $A_-$  is constant on orthogonal hyperbolic surfaces. The scattering singularity is the ellipsoid

$$A_+ = S_+, \quad (74)$$

where

$$S_{\pm} = \frac{1}{2\kappa} (|\vec{l}_2| \pm |\vec{l}_3|). \quad (75)$$

We need one more coordinate. Let  $\phi$  be the azimuthal angle of  $\vec{l}$  in a coordinate system in which the  $z$  axis lies in the direction of  $\vec{l}_2 + \vec{l}_3$  and  $\vec{l}_2$  has zero  $y$  component and a positive

$x$  component. To state this precisely, define unit vectors

$$\begin{aligned}\vec{n}_z &= \frac{\vec{l}_2 + \vec{l}_3}{|\vec{l}_2 + \vec{l}_3|} \\ \vec{n}_y &= \frac{\vec{l}_3 \times \vec{l}_2}{|\vec{l}_3 \times \vec{l}_2|} \\ \vec{n}_x &= \vec{n}_y \times \vec{n}_z.\end{aligned}\tag{76}$$

Then

$$\phi = \arctan(\vec{l} \cdot \vec{n}_y / \vec{l} \cdot \vec{n}_x).\tag{77}$$

The transformation from  $A_+, A_-, \phi$  to  $\vec{l}$  is

$$\vec{l} = \frac{1}{2}(\vec{l}_2 + \vec{l}_3) + l_T \cos \phi \vec{n}_x + l_T \sin \phi \vec{n}_y + z \vec{n}_z,\tag{78}$$

where

$$\begin{aligned}l_T &= \kappa (A_+^2 - 1)^{1/2} (1 - A_-^2)^{1/2} \\ z &= \kappa A_+ A_-.\end{aligned}\tag{79}$$

A straightforward calculation shows that the jacobian of the transformation is given by

$$d\vec{l} = \frac{dA_+ dA_- d\phi}{\rho_{AA\phi}},\tag{80}$$

where

$$\frac{1}{\rho_{AA\phi}} = \kappa^3 (A_+^2 - A_-^2).\tag{81}$$

The factor  $(A_+^2 - A_-^2)$  is convenient. It provides weak singularities in the density of points when  $A_+ \pm A_- \rightarrow 0$ , which corresponds to  $\vec{l} \rightarrow 0$  and  $\vec{l} - \vec{l}_2 - \vec{l}_3 \rightarrow 0$ .

If we sample points in the variables  $\{A_+, A_-, \phi\}$  with a density

$$\rho' = \frac{dN}{dA_+ dA_- d\phi},\tag{82}$$

then the total density of points will be

$$\rho = \rho' \times \rho_{AA\phi},\tag{83}$$

where  $\rho_{AA\phi}$  is given in Eq. (81). We next address the question of what to choose for  $\rho'$ .

## 7.2 The choice of $A_+$ , $A_-$ and $\phi$

With what density

$$\rho' = \frac{dN}{dA_+ dA_- d\phi} \quad (84)$$

should we sample points in the variables  $\{A_+, A_-, \phi\}$ ? There is no unique answer, but consider a density function of the form

$$\rho' = \mathcal{N} \frac{1}{1 - A_-^2 + \tau} \frac{1}{A_+ (|A_+ - S_+| + \lambda)}. \quad (85)$$

Here  $\tau$  and  $\lambda$  are parameters to be specified and the normalization  $\mathcal{N}$  is given by

$$\frac{1}{\mathcal{N}} = \frac{2\pi}{\sqrt{1+\tau}} \ln\left(\frac{\sqrt{1+\tau}+1}{\sqrt{1+\tau}-1}\right) \left\{ \frac{1}{S_+ + \lambda} \ln\left(\frac{S_+[S_+-1+\lambda]}{\lambda}\right) + \frac{1}{S_+ - \lambda} \ln\left(\frac{S_+}{\lambda}\right) \right\}. \quad (86)$$

With this ansatz, there is a high density of points near the scattering singularity surface,  $A_+ = S_+$ . The width of the peak is  $\lambda$ . Thus  $\lambda$  should be matched to the width of the peak in the integrand. If the singularity surface is far from the line  $A_+ = 1$ , the contour deformation is substantial and peak is broad. On the other hand, if the singularity surface is near to the line  $A_+ = 1$ , the contour deformation is small and peak is narrow. I estimate that the width of the peak in the integrand is of order  $(S_+ - 1)^2$  for  $S_+$  near 1. For large  $S_+$  it seems reasonable to choose a width of order  $S_+$ . Thus I take

$$\lambda = \frac{(S_+ - 1)^2}{S_+}. \quad (87)$$

With the function  $\rho'$  in Eq. (85), there is an enhancement of the density of points near  $A_- = \pm 1$ . This enhancement is built into the density in order to provide an extra density of points near where the ellipsoid in Fig. 6 is tangent to the sphere. As explained in Sec. 5, we need a high density of points here when  $\vec{l}_2$  and  $\vec{l}_3$  are nearly collinear, that is when  $S_+$  is close to 1. I arrange for this by taking the parameter  $\tau$  in Eq. (85) to be

$$\tau = \frac{S_+ - 1}{S_+}. \quad (88)$$

It is easy to sample points  $\{A_+, A_-, \phi\}$  with the density  $\rho'$  in Eq. (85) as explained in [6].

### Implementation Notes

To implement the sampling in the variables  $\{A_+, A_-, \phi\}$ , we first sample  $\phi$  in  $0 < \phi < 2\pi$  with a uniform density

$$\rho_\phi = \frac{1}{2\pi} \quad (89)$$

by picking a random variable  $X_\phi$  in  $0 < X_\phi < 1$  and setting

$$\phi = 2\pi X_\phi. \quad (90)$$

Next, we need to choose  $A_-$  with the density

$$\rho_- = \frac{\mathcal{N}_-}{1 - A_-^2 + \tau}. \quad (91)$$

It is convenient to define

$$c = \sqrt{1 + \tau} \quad (92)$$

so that

$$\rho_- = \frac{\mathcal{N}_-}{c^2 - A_-^2}. \quad (93)$$

The normalization is given by

$$\frac{1}{\mathcal{N}_-} = \frac{1}{c} \ln \left( \frac{c+1}{c-1} \right). \quad (94)$$

To sample  $A_-$  with density  $\rho_-$  we pick a random variable  $X_-$  in  $0 < X_- < 1$  and put

$$A_- = c \frac{\exp(c(2X_- - 1)/\mathcal{N}_-) - 1}{\exp(c(2X_- - 1)/\mathcal{N}_-) + 1}. \quad (95)$$

For  $A_+$  we want a density

$$\rho_+ = \frac{\mathcal{N}_+}{A_+(|A_+ - S_+| + \lambda)}. \quad (96)$$

The normalization is

$$\mathcal{N}_+ = \left\{ \frac{1}{S_+ + \lambda} \log \left[ \frac{S_+(S_+ - 1 + \lambda)}{\lambda} \right] + \frac{1}{S_+ - \lambda} \log \left[ \frac{S_+}{\lambda} \right] \right\}^{-1} \quad (97)$$

In order to choose points with this density, we define an auxiliary parameter

$$c_+ = \left\{ 1 + \frac{S_+ + \lambda}{S_+ - \lambda} \frac{\log [S_+/\lambda]}{\log [S_+(S_+ - 1 + \lambda)/\lambda]} \right\}^{-1}. \quad (98)$$

To sample  $A_+$  with density  $\rho_+$  we pick a random variable  $X_+$  in  $0 < X_+ < 1$ . For  $X_+ > c_+$ , we put

$$A_+ = (S_+ - \lambda) \left\{ 1 - \frac{\lambda}{S_+} \exp [(S_+ - \lambda)(X_+ - c_+)/\mathcal{N}_+] \right\}^{-1}. \quad (99)$$

For  $X_+ < c_+$  we put

$$A_+ = (S_+ + \lambda) \left\{ 1 + \frac{\lambda}{S_+} \exp [(S_+ + \lambda)(c_+ - X_+)/\mathcal{N}_+] \right\}^{-1}. \quad (100)$$

The product of  $\rho_\phi$ ,  $\rho_-$  and  $\rho_+$  is  $\rho'$  in Eq. (85).

## 8 Sampling for 2 to 2 ( $t$ ) scattering

In this section, we consider the sampling method associated with 2 to 2 ( $t$ ) scattering. We need to choose points  $\vec{l} \equiv \vec{l}_1$  appropriate to the following case:

A virtual parton with momentum  $\vec{l}_2 + \vec{l}$  scatters from a virtual parton with momentum  $\vec{l}_3 - \vec{l}$  by exchanging a parton with momentum  $\vec{l}$ . Partons with momentum  $\vec{l}_2$  and  $\vec{l}_3$  emerge into the final state.

In this case, there is a scattering singularity surface  $|\vec{l}_2 + \vec{l}| + |\vec{l}_3 - \vec{l}| = |\vec{l}_2| + |\vec{l}_3|$ . There is a singularity on this surface at the point where the momentum  $\vec{l}$  of the exchanged parton vanishes. The density of points should have a matching singularity at this point.

### 8.1 Elliptical coordinates

As in the previous section, we use elliptical coordinates  $A_+, A_-, \phi$ . The role of  $\vec{l}$  in the previous section is now played by  $\vec{l} + \vec{l}_2$ , so the formulas are a little different. We again define  $\kappa$  by  $2\kappa = |\vec{l}_2 + \vec{l}_3|$ . Now, define coordinates  $A_{\pm}$  by

$$A_{\pm} = \frac{1}{2\kappa} (|\vec{l}_2 + \vec{l}| \pm |\vec{l}_3 - \vec{l}|). \quad (101)$$

Then  $1 < A_+$  and  $-1 < A_- < 1$ . Define

$$S_{\pm} = \frac{1}{2\kappa} (|\vec{l}_2| \pm |\vec{l}_3|). \quad (102)$$

The scattering singularity is the ellipsoid

$$A_+ = S_+ \quad (103)$$

while the soft exchange singularity is at

$$\{A_+, A_-\} = \{S_+, S_-\}. \quad (104)$$

We need one more coordinate, an azimuthal angle  $\phi$ . We define unit vectors  $\{\vec{n}_x, \vec{n}_y, \vec{n}_z\}$  according to Eq. (76). Then we define

$$\phi = \arctan \left( (\vec{l}_2 + \vec{l}) \cdot \vec{n}_y / (\vec{l}_2 + \vec{l}) \cdot \vec{n}_x \right). \quad (105)$$

The jacobian of the transformation from  $\vec{l}$  to  $\{A_+, A_-, \phi\}$  is again  $1/\rho_{AA\phi}$  where  $\rho_{AA\phi}$  is given in Eq. (81). If we sample points in the parameters  $\{A_+, A_-, \phi\}$  with a density  $\rho'$  then the total density of points will be  $\rho = \rho' \times \rho_{AA\phi}$ . We next address the question of what to choose for  $\rho'$ .

## 8.2 The choice of $A_+$ , $A_-$ and $\phi$

In this subsection we specify a choice for the density

$$\rho' = \frac{dN}{dA_+ dA_- d\phi} \quad (106)$$

with which we sample in the variables  $\{A_+, A_-, \phi\}$ . We begin by recognizing that we face two challenges. First, we would like to have a concentration of points near the surface  $A_+ = S_+$  with an especially high density near  $A_- = \pm 1$  if  $S_+$  is near 1, as discussed with respect to the sampling for  $\mathcal{Z}$  to  $\mathcal{Z}(s)$ . The second challenge is to make  $\rho'$  appropriately singular at  $\{A_+, A_-, \phi\} = \{S_+, S_-, 0\}$ . We thus take  $\rho'$  to have two parts

$$\rho' = \alpha_{2t} \rho_s + (1 - \alpha_{2t}) \rho_t, \quad (107)$$

where  $\alpha_{2t}$  is a fixed parameter with  $0 < \alpha_{2t} < 1$ . We take  $\rho_s$  to be given by the density (85) for the sampling for  $\mathcal{Z}$  to  $\mathcal{Z}(s)$ . Then we have met the first challenge. It remains to design  $\rho_t$  to address the second challenge.

The main idea is that there is a scattering singularity surface at  $A_+ = S_+$ , so that the integrand has a factor

$$\frac{1}{A_+ - S_+ + i\eta} \quad (108)$$

where  $\eta$  is the amount of deformation of the  $S_+$  contour. The amount of contour deformation vanishes at the soft exchange singularity at  $\{A_+, A_-, \phi\} = \{S_+, S_-, 0\}$  and, near to this point,  $\eta$  is proportional to the square of the distance to  $\{S_+, S_-, 0\}$ . Thus, on the surface  $A_+ = S_+$  near to the soft exchange singularity, we can estimate  $\eta$  as  $\omega^2$  where

$$\omega \equiv |A_- - S_-| + |\phi|/\pi. \quad (109)$$

There is another factor of  $1/\omega$  that arises from the propagator of the exchanged parton after we take real-virtual cancellations into account, as explained in detail in Ref. [4]. Thus the absolute value of the integrand has a factor that can be estimated as

$$\frac{1}{\omega |A_+ - S_+|} \quad (110)$$

for  $\omega \ll 1$  and  $\omega^2 \ll |A_+ - S_+| \ll \omega$ . We want  $\rho_t$  to have a singularity of the same nature, so that the integrand divided by the density of points is singularity free. Thus we take

$$\rho_t = \frac{\mathcal{A}}{[|A_+ - S_+| + \beta_{2t} S_+ \omega^2][|A_+ - S_+| + \beta_{2t} \gamma_{2t} S_+ \omega]}. \quad (111)$$

Here  $\beta_{2t}$  and  $\gamma_{2t}$  are fixed parameters and  $\mathcal{A}$  is a rather complicated function of  $A_-$  and  $\phi$  (described below) that is of secondary importance. The main point is that  $\rho_t$  behaves like (110), with cutoffs when  $|A_+ - S_+|$  gets to be smaller than  $\omega^2$  or larger than  $\omega$ .

We have thus given  $\rho_t$  an actual singularity at the point  $\{A_+, A_-, \phi\} = \{S_+, S_-, 0\}$ . This singularity in  $\rho_t$  has a special structure such that matches the structure of the integrand  $f$ , so that  $f/\rho_t$  is finite in the neighborhood of the soft exchange singularity. This point, which is important for the convergence of the numerical integration, was described in some detail in Ref. [4]. In that paper, however, the construction was not as nice as one would like because the ellipsoidal coordinates were not used and the “ridgeline” of  $\rho$  was placed on the tangent plane to the ellipsoid rather than on the ellipsoid itself.

To sample points with the density  $\rho_t$  of Eq. (111), we sample first in  $\phi$  with a density proportional to  $\ln^2(\pi\gamma_{2t}/|\phi|)$ . Then, with  $\phi$  chosen, we sample in  $A_-$  with a density proportional to  $\log(\gamma_{2t}/\omega)/\omega$ . Finally, having chosen  $\phi$  and  $A_-$ , we sample in  $A_+$  with a density proportional to the right hand side of Eq. (111). Taking into account the normalization conditions, this gives the result in Eq. (111) with

$$\begin{aligned} \frac{1}{\mathcal{A}} &= \frac{4\pi}{S_+\beta} [\ln^2(\gamma_{2t}) + 2\ln(\gamma_{2t}) + 2] \frac{1}{\gamma_{2t} - \omega} \\ &\quad \times \left\{ 1 + \frac{1}{2\ln(\gamma_{2t}/\omega)} \ln \left( \frac{S_+ - 1 + \beta_{2t}S_+\omega^2}{S_+ - 1 + \beta_{2t}\gamma_{2t}S_+\omega} \right) \right\} \\ &\quad \times \left\{ 1 - \frac{1}{2\ln^2(\pi\gamma_{2t}/|\phi|)} \left[ \ln^2 \left( \frac{\gamma_{2t}}{1 + S_- + |\phi|/\pi} \right) + \ln^2 \left( \frac{\gamma_{2t}}{1 - S_- + |\phi|/\pi} \right) \right] \right\}. \end{aligned} \quad (112)$$

The function  $\mathcal{A}$  may be a bit complicated, but it is quite benign. In particular,  $\mathcal{A}$  is not singular or zero anywhere provided that  $\gamma_{2t} > \omega$  holds everywhere. This requires that  $\gamma_{2t} > 3$ .

### Implementation Notes

We begin the explanation with the choice of  $A_+$ , assuming that  $A_-$  and  $\phi$  have already been chosen. Then we take the density of points in  $A_+$  to have the form

$$\begin{aligned} \rho_+ &= \frac{\mathcal{N}_+\beta_{2t}S_+\omega(\gamma_{2t} - \omega)}{(|A_+ - S_+| + \beta_{2t}S_+\omega^2)(|A_+ - S_+| + \beta_{2t}\gamma_{2t}S_+\omega)} \\ &= \frac{\mathcal{N}_+}{|A_+ - S_+| + \beta_{2t}S_+\omega^2} - \frac{\mathcal{N}_+}{|A_+ - S_+| + \beta_{2t}\gamma_{2t}S_+\omega}. \end{aligned} \quad (113)$$

Here  $\mathcal{N}_+$  is the normalization such that  $\int dA_+ \rho_+ = 1$ . This density produces the properties we want provided that we can choose the densities of  $A_-$  and  $\phi$  so as to cancel the factor  $\omega$  (along with a factor  $1/\ln \omega$  that appears in  $\mathcal{N}_+$ ) in the numerator in the first equation above.

We will need the indefinite integral of  $\rho_+$ :

$$\int_{S_+}^{A_+} d\bar{A}_+ \rho_+(\bar{A}_+) = \mathcal{N}_+ \text{sign}(A_+ - S_+) \ln \left( \frac{\gamma_{2t}}{\omega} \frac{|A_+ - S_+| + \beta_{2t}S_+\omega^2}{|A_+ - S_+| + \beta_{2t}\gamma_{2t}S_+\omega} \right). \quad (114)$$

Using this result we calculate

$$\frac{1}{\mathcal{N}_+} = \ln \left( \frac{\gamma_{2t}^2}{\omega^2} \frac{S_+ - 1 + \beta_{2t}S_+\omega^2}{S_+ - 1 + \beta_{2t}\gamma_{2t}S_+\omega} \right). \quad (115)$$

Notice the logarithmic singularity for  $\omega \rightarrow 0$ .

Next we define

$$X_+ = \int_1^{A_+} d\bar{A}_+ \rho_+(\bar{A}_+). \quad (116)$$

Evidently if we choose values of  $X_+$  at random with a uniform distribution in  $0 < X_+ < 1$ , then the corresponding  $A_+$  values will have a random distribution in  $1 < A_+ < \infty$  with density  $\rho_+$ . In order to write this mapping explicitly we define the critical value of  $X_+$  that corresponds to  $A_+ = S_+$ ,

$$c_+ = \int_1^{S_+} d\bar{A}_+ \rho_+(\bar{A}_+) \quad (117)$$

That is

$$c_+ = \mathcal{N}_+ \ln \left( \frac{\gamma_{2t}}{\omega} \frac{S_+ - 1 + \beta_{2t} S_+ \omega^2}{S_+ - 1 + \beta_{2t} \gamma_{2t} S_+ \omega} \right). \quad (118)$$

Also

$$1 - c_+ = \mathcal{N}_+ \ln \left( \frac{\gamma_{2t}}{\omega} \right). \quad (119)$$

Then

$$X_+ - c_+ = \int_{S_+}^{A_+} d\bar{A}_+ \rho_+(\bar{A}_+). \quad (120)$$

That is

$$X_+ - c_+ = \mathcal{N}_+ \text{sign}(A_+ - S_+) \ln \left( \frac{\gamma_{2t}}{\omega} \frac{|A_+ - S_+| + \beta_{2t} S_+ \omega^2}{|A_+ - S_+| + \beta_{2t} \gamma_{2t} S_+ \omega} \right). \quad (121)$$

We can solve this for  $A_+$ :

$$A_+ = S_+ + \text{sign}(X_+ - c_+) \beta_{2t} S_+ \omega^2 \frac{\exp(|X_+ - c_+|/\mathcal{N}_+) - 1}{1 - (\omega/\gamma_{2t}) \exp(|X_+ - c_+|/\mathcal{N}_+)} \quad (122)$$

There are two other forms for this, depending on the sign of  $X_+ - c_+$ . For  $X_+ < c_+$  we find

$$A_+ - 1 = \frac{a b F(X_+)}{(\gamma_{2t} - \omega) \beta_{2t} S_+ \omega + a F(X_+)} \quad (123)$$

where

$$\begin{aligned} a &= S_+ - 1 + \beta_{2t} S_+ \omega^2, \\ b &= S_+ - 1 + \beta_{2t} \gamma_{2t} S_+ \omega, \end{aligned} \quad (124)$$

and

$$F(x) = 1 - e^{-x/\mathcal{N}_+}. \quad (125)$$

For  $X_+ > c_+$  we find

$$A_+ - S_+ = \beta_{2t} S_+ \omega \frac{(\gamma_{2t} - \omega) - \gamma_{2t} F(1 - X_+)}{F(1 - X_+)}. \quad (126)$$

These forms are evidently superior in the case that  $\omega \ll 1$  and  $X_+$  is near to 0 or 1.

We proceed with the explanation of the choice of  $A_-$ , assuming that  $\phi$  has already been chosen. Since  $\rho_+$  contains a factor of  $\omega = |A_- - S_-| + |\phi|/\pi$  and a factor of  $1/\ln(\omega)$  that we do not want, we want to choose  $A_-$  with a density  $\rho_-$  containing the inverse of these factors. We choose

$$\rho_-(A_-) = \frac{\mathcal{N}_- \ln(\gamma_{2t}/[|A_- - S_-| + |\phi|/\pi])}{|A_- - S_-| + |\phi|/\pi}. \quad (127)$$

The normalization factor  $\mathcal{N}_-$  is defined so that  $\int dA_- \rho_- = 1$ .

We need the indefinite integral

$$\int_{S_-}^{A_-} d\bar{A}_- \rho_-(\bar{A}_-) = \frac{\mathcal{N}_-}{2} \text{sign}(A_- - S_-) \left\{ \ln^2 \left( \frac{\gamma_{2t}\pi}{|\phi|} \right) - \ln^2 \left( \frac{\gamma_{2t}}{|A_- - S_-| + |\phi|/\pi} \right) \right\}. \quad (128)$$

Using this result we calculate

$$\frac{1}{\mathcal{N}_-} = \ln^2 \left( \frac{\pi\gamma_{2t}}{|\phi|} \right) - \frac{1}{2} \ln^2 \left( \frac{\gamma_{2t}}{1 + S_- + |\phi|/\pi} \right) - \frac{1}{2} \ln^2 \left( \frac{\gamma_{2t}}{1 - S_- + |\phi|/\pi} \right). \quad (129)$$

Notice the logarithmic singularity for  $|\phi| \rightarrow 0$ .

Next we define

$$X_- = \int_{-1}^{A_-} d\bar{A}_- \rho_-(\bar{A}_-). \quad (130)$$

Evidently if we choose values of  $X_-$  at random with a uniform distribution in  $0 < X_- < 1$ , then the corresponding  $A_-$  values will have a random distribution in  $-1 < A_- < 1$  with density  $\rho_-$ . In order to write this mapping explicitly we define the critical value of  $X_-$  that corresponds to  $A_- = S_-$ ,

$$c_- = \int_{-1}^{S_-} d\bar{A}_- \rho_-(\bar{A}_-). \quad (131)$$

That is

$$c_- = \frac{\mathcal{N}_-}{2} \left\{ \ln^2 \left( \frac{\gamma_{2t}\pi}{|\phi|} \right) - \ln^2 \left( \frac{\gamma_{2t}}{1 + S_- + |\phi|/\pi} \right) \right\}. \quad (132)$$

Also

$$1 - c_- = \frac{\mathcal{N}_-}{2} \left\{ \ln^2 \left( \frac{\gamma_{2t}\pi}{|\phi|} \right) - \ln^2 \left( \frac{\gamma_{2t}}{1 - S_- + |\phi|/\pi} \right) \right\}. \quad (133)$$

Then

$$X_- - c_- = \int_{S_-}^{A_-} d\bar{A}_- \rho_-(\bar{A}_-). \quad (134)$$

That is

$$X_- - c_- = \frac{\mathcal{N}_-}{2} \text{sign}(A_- - S_-) \left\{ \ln^2 \left( \frac{\gamma_{2t}\pi}{|\phi|} \right) - \ln^2 \left( \frac{\gamma_{2t}}{|A_- - S_-| + |\phi|/\pi} \right) \right\}. \quad (135)$$

We can solve this for  $A_-$ :

$$A_- = S_- + \text{sign}(X_- - c_-) \left\{ \gamma_{2t} \exp \left( - \left[ \ln^2 \left( \frac{\gamma_{2t}\pi}{|\phi|} \right) - \frac{2}{\mathcal{N}_-} |X_- - c_-| \right]^{1/2} \right) - \frac{|\phi|}{\pi} \right\}. \quad (136)$$

There are two another form for this, depending on the sign of  $X_- - c_-$ . For  $X_- < c_-$ , we find

$$A_- = S_- - \gamma_{2t} \exp \left( - \left[ \frac{2X_-}{\mathcal{N}_-} + \ln^2 \left( \frac{\gamma_{2t}}{1 + S_- + |\phi|/\pi} \right) \right]^{1/2} \right) + \frac{|\phi|}{\pi}. \quad (137)$$

For  $X_- > c_-$ , we find

$$A_- = S_- + \gamma_{2t} \exp \left( - \left[ \frac{2(1 - X_-)}{\mathcal{N}_-} + \ln^2 \left( \frac{\gamma_{2t}}{1 - S_- + |\phi|/\pi} \right) \right]^{1/2} \right) - \frac{|\phi|}{\pi}. \quad (138)$$

These forms are evidently superior in the case that  $X_-$  is near to 0 or 1.

We conclude with the explanation of the choice of  $\phi$ . Since  $\rho_-$  contains a factor of  $1/\ln^2(|\phi|)$  that we do not want, we choose  $\phi$  in  $-\pi < \phi < \pi$  with a density

$$\rho_\phi = \mathcal{N}_\phi \ln^2 \left( \frac{|\phi|}{\pi \gamma_{2t}} \right) \quad (139)$$

The normalization here is

$$\mathcal{N}_\phi = \frac{1}{2\pi\gamma_{2t}} \frac{1}{h(1/\gamma_{2t})}, \quad (140)$$

where  $h$  is the function

$$h(y) = y (\ln^2(y) - 2\ln y + 2). \quad (141)$$

Next we define

$$X_\phi = \int_{-\pi}^\phi d\bar{\phi} \rho_\phi(\bar{\phi}). \quad (142)$$

Evidently if we choose values of  $X_-$  at random with a uniform distribution in  $0 < X_- < 1$ , then the corresponding  $A_-$  values will have a random distribution in  $-1 < A_- < 1$  with density  $\rho_-$ . The relation (142) is

$$2X_\phi - 1 = \frac{\text{sign}(\phi)}{h(1/\gamma_{2t})} h \left( \frac{|\phi|}{\pi \gamma_{2t}} \right). \quad (143)$$

Solving for  $\phi$  gives

$$\phi = \text{sign}(2X_\phi - 1) \pi \gamma_{2t} h^{-1}(|2X_\phi - 1|h(1/\gamma_{2t})), \quad (144)$$

where  $y = h^{-1}(z)$  is the solution to  $z = h(y)$ . (It is easy to solve this equation numerically to very high accuracy.)

The transformation from  $A_+, A_-, \phi$  to  $\vec{l}$  is

$$\vec{l} = \frac{1}{2}(\vec{l}_3 - \vec{l}_2) + l_T \cos \phi \vec{n}_x + l_T \sin \phi \vec{n}_y + z \vec{n}_z \quad (145)$$

where

$$\begin{aligned} l_T &= \kappa (A_+^2 - 1)^{1/2} (1 - A_-^2)^{1/2} \\ z &= \kappa A_+ A_- \end{aligned} \quad (146)$$

This form for  $\vec{l}$  is not accurate near the soft singularity,  $\vec{l} = 0$ . Instead, we define

$$A_{\pm} = S_{\pm} + \Delta A_{\pm}. \quad (147)$$

Then we write

$$\begin{aligned} l_T &= l_{T0} + \Delta l_T, \\ z &= z_0 + \Delta z. \end{aligned} \quad (148)$$

where

$$\begin{aligned} l_{T0} &= \kappa (S_+^2 - 1)^{1/2} (1 - S_-^2)^{1/2}, \\ z_0 &= \kappa S_+ S_-. \end{aligned} \quad (149)$$

Then  $\Delta l_T$  is given by

$$\Delta l_T = l_{T0} G(\zeta) \quad (150)$$

where

$$G(\zeta) = [1 + \zeta]^{1/2} - 1 \quad (151)$$

and

$$\begin{aligned} \zeta &= \Delta A_+ \frac{2S_+ + \Delta A_+}{S_+^2 - 1} \\ &\quad - \Delta A_- \frac{2S_- + \Delta A_-}{1 - S_-^2} \\ &\quad - \Delta A_+ \Delta A_- \frac{2S_+ + \Delta A_+}{S_+^2 - 1} \frac{2S_- + \Delta A_-}{1 - S_-^2}. \end{aligned} \quad (152)$$

For  $\Delta z$  we have

$$\Delta z = \kappa (\Delta A_+ S_- + \Delta A_- S_+ + \Delta A_+ \Delta A_-). \quad (153)$$

Since  $\vec{l} = 0$  when  $\Delta A_+ = 0$ ,  $\Delta A_- = 0$ , and  $\phi = 0$ , we have

$$\vec{l} = [\Delta l_T \cos \phi - l_{T0}(1 - \cos \phi)] \vec{n}_x + l_T \sin \phi \vec{n}_y + \Delta z \vec{n}_z. \quad (154)$$

## 9 Sampling for 2 to 3 scattering

In this section, we consider the sampling method for the third type of scattering singularity surface. We need to choose points  $\vec{l} \equiv \vec{l}_1$  appropriate to the following case:

A virtual parton with momentum  $\vec{l}$  collides with a virtual parton with momentum  $-\vec{l}$  to produce a final state with partons carrying momenta  $\vec{l}_2$ ,  $\vec{l}_3$ , and  $-\vec{l}_2 - \vec{l}_3$ .

In this case, the scattering surface is the sphere  $2|\vec{l}| = |\vec{l}_2| + |\vec{l}_3| + |\vec{l}_2 + \vec{l}_3|$ . The density of points should be large on this surface. There is no special point embedded in the surface where the density of points needs to be singular. However, the density should be enhanced near the point of this sphere where it intersects the ellipsoid in Fig. 6 or the narrower of the two ellipsoids in Fig. 8.

Since the scattering singularity surface is a sphere, we use spherical polar coordinates  $\{r, \cos \theta, \phi\}$  to describe  $\vec{l}$ . We choose the  $\theta = 0$  axis along a certain direction  $\vec{P}_C$ . In the case (d) illustrated in Fig. 5, we define  $\vec{P}_C = -\vec{p}_3$ . In the case (e) illustrated in Fig. 7, we define  $\vec{P}_C = \vec{p}_1$  if  $|\vec{p}_1| > |\vec{p}_3|$  or  $\vec{P}_C = -\vec{p}_3$  if  $|\vec{p}_3| > |\vec{p}_1|$ .

The jacobian of the transformation from  $\vec{l}$  to  $\{r, \cos \theta, \phi\}$  is

$$d\vec{l} = \frac{dr d\cos \theta d\phi}{\rho_{r\theta\phi}}, \quad (155)$$

where

$$\rho_{r\theta\phi} = \frac{1}{r^2}. \quad (156)$$

If we sample points in the variables  $\{r, \cos \theta, \phi\}$  with a density

$$\rho' = \frac{dN}{dr d\cos \theta d\phi}, \quad (157)$$

then the total density of points will be

$$\rho = \rho' \times \rho_{r\theta\phi}. \quad (158)$$

We now address the question of how to choose  $\rho'$ . Our analysis follows closely that in Sec. 8.2. The main idea is that there is a scattering singularity surface at  $r = S$ , where

$$S = \frac{1}{2}(|\vec{l}_2| + |\vec{l}_3| + |\vec{l}_2 + \vec{l}_3|). \quad (159)$$

Thus the integrand has a factor

$$\frac{1}{(r/S) - 1 + i\eta}, \quad (160)$$

where  $\eta$  is the amount of deformation of the  $r/S$  contour. The amount of contour deformation vanishes quadratically as  $\{r, \cos \theta\}$  approaches  $\{S_C, 1\}$ , where

$$S_C = |\vec{P}_C|. \quad (161)$$

The point  $\{S_C, 1\}$  is the point  $\vec{l} = \vec{P}_C$ . That is,  $\vec{l} = -\vec{p}_3$  in Fig. 6 or in Fig. 8 when  $|\vec{p}_3| > |\vec{p}_1|$ . Thus, on the surface  $r = S$ , the amount of deformation  $\eta$  can be estimated as  $\Delta^2$  where

$$\Delta = \frac{1}{3} \sqrt{(1 - S_C/S)^2 + (1 - \cos \theta)}. \quad (162)$$

Thus the absolute value of the integrand has a factor that can be estimated as

$$\frac{1}{|(r/S) - 1|} \quad (163)$$

for  $\Delta \ll 1$  and  $\Delta^2 \ll |(r/S) - 1| \ll \Delta$ . We want  $\rho'$  to have a singularity of the same nature, so that the integrand divided by the density of points is singularity free. Furthermore, we would like  $\rho'$  to have an extra factor of  $1/\Delta^2$  to cancel the factor from the singularity associated with the narrow ellipsoid in Fig. 5 as we approach  $\theta = 0$ . Thus we take

$$\rho' = \frac{\mathcal{B}}{\Delta (|(r/S) - 1| + \alpha_3 \Delta^2) (|(r/S) - 1| + \alpha_3 \Delta)}, \quad (164)$$

where  $\alpha_3$  is a fixed parameter and where  $\mathcal{B}$  is a rather complicated but nonsingular function that gets the normalization right:

$$\mathcal{B} = \frac{\alpha_3(1 - \Delta)}{18\pi S} \left[ \ln \left( \frac{1}{\Delta^2} \frac{1 + \alpha_3 \Delta^2}{1 + \alpha_3 \Delta} \right) \right]^{-1} \left[ \ln \left( 1 + \frac{2}{(1 - S_C/S)^2} \right) \right]^{-1}. \quad (165)$$

#### Implementation Notes

We begin the explanation with the choice of  $r$ , assuming that  $\cos \theta$  and  $\phi$  have already been chosen. Then we take the density of points in  $r$  to have the form

$$\rho_r = \frac{\alpha_3 \mathcal{N}_r}{S} \frac{\Delta(1 - \Delta)}{(|(r/S) - 1| + \alpha_3 \Delta^2)(|(r/S) - 1| + \alpha_3 \Delta)}. \quad (166)$$

The normalization, chosen so that  $\int dr \rho_r = 1$ , is

$$\mathcal{N}_r = \left[ \ln \left( \frac{1}{\Delta^2} \frac{1 + \alpha_3 \Delta^2}{1 + \alpha_3 \Delta} \right) \right]^{-1}. \quad (167)$$

In order to choose points with this density, we choose  $X_r$  at random in  $0 < X_r < 1$ . We define

$$c_r = \ln \left( \frac{1}{\Delta} \frac{1 + \alpha_3 \Delta^2}{1 + \alpha_3 \Delta} \right) / \ln \left( \frac{1}{\Delta^2} \frac{1 + \alpha_3 \Delta^2}{1 + \alpha_3 \Delta} \right). \quad (168)$$

For  $X > c_r$  we put

$$r = S + \alpha_3 S \Delta^2 \frac{\exp[(X_r - c_r)/\mathcal{N}_r] - 1}{1 - \Delta \exp[(X_r - c_r)/\mathcal{N}_r]}. \quad (169)$$

For  $X < c_r$  we put

$$r = S - \alpha_3 S \Delta^2 \frac{\exp[(c_r - X_r)/\mathcal{N}_r] - 1}{1 - \Delta \exp[(c_r - X_r)/\mathcal{N}_r]}. \quad (170)$$

We now turn to the sampling in  $\cos \theta$ . For the density of points in  $\cos \theta$  we take:

$$\rho_\theta = \frac{\mathcal{N}_\theta}{9\Delta^2} = \frac{\mathcal{N}_\theta}{(1 - S_C/S)^2 + (1 - \cos \theta)}. \quad (171)$$

The normalization, chosen so that  $\int d \cos \theta \rho_\theta = 1$ , is

$$\mathcal{N}_\theta = \left[ \ln \left( 1 + \frac{2}{(1 - S_C/S)^2} \right) \right]^{-1}. \quad (172)$$

In order to choose points with this density, we choose  $X_\theta$  at random in  $0 < X_\theta < 1$ . Then we put

$$\cos \theta = 1 - (1 - S_C/S)^2 [\exp(X_\theta/\mathcal{N}_\theta) - 1]. \quad (173)$$

Finally, we sample  $\phi$  in  $0 < \phi < 2\pi$  with a uniform density

$$\rho_\phi = \frac{1}{2\pi} \quad (174)$$

by picking a random variable  $X_\phi$  in  $0 < X_\phi < 1$  and setting

$$\phi = 2\pi X_\phi. \quad (175)$$

The product of  $\rho_r$ ,  $\rho_\theta$  and  $\rho_\phi$  is  $\rho'$  in Eq. (164).

---

## 10 Sampling for 2 to 1 scattering

In this section, we consider the sampling method for the fourth type of scattering singularity surface:

A virtual parton with momentum  $\vec{l}$  combines with a virtual parton with momentum  $\vec{l}_2 - \vec{l}$  to produce an on shell parton with momentum  $\vec{l}_2$  that enters the final state.

As mentioned in Sec. 5, the 2 to 1 scattering singularity surface is exceptional in that there is no singularity except for the two singular points at  $\vec{l} = 0$  and  $\vec{l}_2 - \vec{l} = 0$ . Typically a 2 to 1 scattering subdiagram is part of a 2 to 2 ( $s$ ) or 2 to 2 ( $t$ ) scattering subdiagram and the two singularities are provided for by the 2 to 2 ( $s$ ) or 2 to 2 ( $t$ ) sampling methods. The exception is in the case of a self-energy subgraph that is connected to a final state parton. In this case, the 2 to 2 ( $t$ ), 2 to 2 ( $s$ ), and 2 to 3 sampling methods do not apply and we

need an explicit *2 to 1* sampling method. Thus we apply a *2 to 1* sampling method only in the case of a self-energy subgraph connected to a final state parton.

We will choose  $\vec{l}$  with a density that is a linear combination of five densities:

$$\rho(\vec{l}) = \alpha_{1a} \rho_a(\vec{l}) + \alpha_{1b} \rho_b(\vec{l}) + \alpha_{1a} \rho_a(\vec{l} - \vec{l}_2) + \alpha_{1b} \rho_b(\vec{l} - \vec{l}_2) + (1 - 2\alpha_{1a} - 2\alpha_{1b}) \rho_c(\vec{l}). \quad (176)$$

Here  $\alpha_{1a}$  and  $\alpha_{1b}$  are fixed positive parameters with  $(1 - 2\alpha_{1a} - 2\alpha_{1b})$  also positive.

For  $\rho_a(\vec{l})$  we take

$$\rho_a(\vec{l}) = \frac{|\vec{l}_2|}{4\pi} \frac{1}{\vec{l}^2} \frac{1}{(|\vec{l}| + |\vec{l}_2|)^2}. \quad (177)$$

The density  $\rho_b$  is a simple variation on this with  $|\vec{l}_2|$  replaced by a scale  $M$ :

$$\rho_b(\vec{l}) = \frac{M}{4\pi} \frac{1}{\vec{l}^2} \frac{1}{(|\vec{l}| + M)^2}. \quad (178)$$

Here  $M = (|\vec{l}_2| + |\vec{l}_3| + |\vec{l}_2 + \vec{l}_3|)/3$ , where the momenta of the particles in the final state are  $\vec{l}_2$ ,  $\vec{l}_3$ , and  $-\vec{l}_2 - \vec{l}_3$ . The  $\rho_a$  and  $\rho_b$  terms provide singularities at  $\vec{l}^2 = 0$  and  $(\vec{l}_2 - \vec{l})^2 = 0$ .

The  $\rho_c$  term provides a non-singular density of points in the neighborhood of the collinear line  $\vec{l} = x\vec{l}_2$  with  $0 < x < 1$ . For  $\rho_c(\vec{l})$  we take

$$\rho_c(\vec{l}) = \frac{\beta_1 \gamma_1^2 |\vec{l}_2|}{2\pi} \frac{1}{\sqrt{\beta_1^2 + (x - 1/2)^2}} \frac{1}{(\sqrt{\beta_1^2 + (x - 1/2)^2} + \beta_1) (\vec{l}_T^2 + \gamma_1^2 \vec{l}_2^2)^2}. \quad (179)$$

Here  $\beta_1$  and  $\gamma_1$  are fixed parameters and  $x$  and  $\vec{l}_T$  are defined by writing

$$\vec{l} = x\vec{l}_2 + \vec{l}_T, \quad (180)$$

where  $\vec{l}_T$  is the part of  $\vec{l}$  that is orthogonal to  $\vec{l}_2$ .

#### Implementation Notes

It is easy to generate points with each of the desired densities. First, we decide which of the three density functions to use at random with the probabilities  $\alpha_{1a}$ ,  $\alpha_{1b}$ ,  $\alpha_{1a}$ ,  $\alpha_{1b}$ , and  $1 - 2\alpha_{1a} - 2\alpha_{1b}$  respectively. Then we generate a point for the chosen density function.

To generate points with the density  $\rho_a(\vec{l})$ , we write  $\vec{l}$  in terms of spherical polar coordinates  $\{r, \theta, \phi\}$ . We choose  $\{\theta, \phi\}$  at random on the unit sphere. We choose  $r$  according to the following general scheme. Choose  $X_r$  at random in  $0 < X_r < 1$ . Then put

$$r = K_0 \left( \frac{1}{X_r^{A/B}} - 1 \right)^{1/A}, \quad (181)$$

where  $A$  and  $B$  are parameters to be fixed in a moment and  $K_0$  is a scale setting parameter. The corresponding density is

$$\rho_r = \frac{1}{dr/dX_r} = BK_0^B r^{A-1} (r^A + K_0^A)^{-1-B/A}. \quad (182)$$

We take  $A = 1$  and  $B = 1$ . For the scale setting parameter we take  $K_0 = |\vec{l}_2|$ . Thus

$$r = |\vec{l}_2| \left( \frac{1}{X_r} - 1 \right) \quad (183)$$

and

$$\rho_r = |\vec{l}_2| (r + |\vec{l}_2|)^{-2}. \quad (184)$$

Then, using  $d\vec{l} = r^2 dr d\theta d\phi$  we get Eq. (177) for  $\rho_a$ .

To generate points with the density  $\rho_b(\vec{l})$ , we follow the same procedure with  $K_0 = M = (|\vec{l}_2| + |\vec{l}_3| + |\vec{l}_2 + \vec{l}_3|)/3$  instead of  $K_0 = |\vec{l}_2|$ .

To generate points with the density  $\rho_c(\vec{l})$ , we write  $\vec{l} = x\vec{l}_2 + \vec{l}_T$  as in Eq. (180). We choose  $x$  according to

$$x = \frac{1}{2} + \beta_1 \frac{X_x - \frac{1}{2}}{X_x(1 - X_x)}, \quad (185)$$

where  $X_x$  is a random variable in  $0 < X_x < 1$ . The corresponding density is

$$\rho_x = \frac{\beta_1}{2\sqrt{\beta_1^2 + (x - \frac{1}{2})^2}(\sqrt{\beta_1^2 + (x - \frac{1}{2})^2} + \beta_1)}. \quad (186)$$

We write  $\vec{l}_T$  in terms of its magnitude  $l_T$  and a polar angle (around the  $\vec{l}_2$  axis)  $\phi$ . We choose  $\phi$  at random in  $0 < \phi < 2\pi$ , with density  $1/2\pi$ . We choose  $l_T$  according to the general scheme discussed above with the choice  $A = 2$ ,  $B = 2$  and with a scale parameter  $K_0 = \gamma_1 |\vec{l}_2|$ . Thus

$$l_T = \gamma_1 |\vec{l}_2| \left( \frac{1}{X_T} - 1 \right)^{1/2}, \quad (187)$$

where  $X_T$  is another random variable in  $0 < X_T < 1$ . The corresponding density is then

$$\rho_T = 2\gamma_1^2 l_2^2 l_T (l_T^2 + \gamma_1^2 l_2^2)^{-2}. \quad (188)$$

Putting this together with the use of  $d\vec{l} = |\vec{l}_2| dx l_T dl_T d\phi$  we obtain Eq. (179) for  $\rho_c$ .

## 11 Structure of Singularities

We now turn to an examination of the structure of the singularities arising from virtual graphs, which will lead us to an analysis of the required contour deformations. We first consider the case of a virtual loop on the left hand side of the final state cut. Later we will consider the case of a virtual loop on the right hand side of the final state cut.

Consider a virtual loop that has exactly one vertex that is not connected to a propagator that enters the final state (a cut propagator). We choose a direction around the loop by an arbitrary convention. Then we can number the propagators around the loop  $J = 1, 2, \dots, N_L$  starting at the special vertex and moving around the loop in the positive direction. Call the corresponding momenta  $l_J^\mu$ . Then the  $J$ th propagator around the loop has index  $P = R(J)$ , with  $\epsilon(J) = \pm 1$  giving the positive direction for propagator  $P$  relative to the positive direction around the loop. That is,  $k_{R(J)}^\mu = \epsilon(J) l_J^\mu$ .

As discussed earlier, we divide the integral into several terms. In a typical term, one of the loop propagators, call it  $J^*$ , is “cut.” That is, we replace the propagator  $1/(l_{J^*}^2 + i\epsilon)$  by  $1/(2|\vec{l}_{J^*}|)$  and set  $l_{J^*}^0 = |\vec{l}_{J^*}|$  in the rest of the integrand. What kind of singularities does this give us for the other loop propagators? Let us examine each case in turn.

- $J = J^* - 1$ : We have  $l_{J^*-1}^\mu = l_{J^*}^\mu + Q^\mu$  where  $Q^2 = 0$  and  $Q^0 > 0$ . Thus

$$l_{J^*-1}^2 + i\epsilon = 2l_{J^*}^\mu Q_\mu + i\epsilon = 2|\vec{l}_{J^*}| |\vec{Q}| (1 - \cos\theta), \quad (189)$$

where  $\theta$  is the angle between  $\vec{l}_{J^*}$  and  $\vec{Q}$ . We thus have singularities when  $\vec{l}_{J^*}$  is soft and when it is collinear to  $\vec{Q}$ . Since these are endpoint singularities, there is no  $i\epsilon$  prescription for them.

- $J = J^* + 1$ : We have  $l_{J^*+1}^\mu = l_{J^*}^\mu - Q^\mu$  where  $Q^2 = 0$  and  $Q^0 > 0$ . Thus

$$l_{J^*+1}^2 + i\epsilon = -2l_{J^*}^\mu Q_\mu + i\epsilon = -2|\vec{l}_{J^*}| |\vec{Q}| (1 - \cos\theta), \quad (190)$$

where  $\theta$  is the angle between  $\vec{l}_{J^*}$  and  $\vec{Q}$ . We thus have singularities when  $\vec{l}_{J^*}$  is soft and when it is collinear to  $\vec{Q}$ . Again, there is no  $i\epsilon$  prescription.

- $J = J^* - n$  with  $n > 1$ : We have  $l_{J^*-n}^\mu = l_{J^*}^\mu + Q^\mu$  where  $Q^2 > 0$  and  $Q^0 > 0$ . Thus

$$l_{J^*-n}^2 + i\epsilon = 2l_{J^*}^\mu Q_\mu + Q^\mu Q_\mu + i\epsilon = 2|\vec{l}_{J^*}|(Q^0 - |\vec{Q}| \cos\theta) + Q^2, \quad (191)$$

where  $\theta$  is the angle between  $\vec{l}_{J^*}$  and  $\vec{Q}$ . Since  $Q^0 > |\vec{Q}|$  and  $Q^2 > 0$ , this factor is positive definite and does not give rise to a singularity.

- $J = J^* + n$  with  $n > 1$ : We have  $l_{J^*+n}^\mu = l_{J^*}^\mu - Q^\mu$  where  $Q^2 > 0$  and  $Q^0 > 0$ . Thus

$$l_{J^*+n}^2 + i\epsilon = -2l_{J^*}^\mu Q_\mu + Q^\mu Q_\mu + i\epsilon = -2|\vec{l}_{J^*}|(Q^0 - |\vec{Q}| \cos\theta) + Q^2 + i\epsilon, \quad (192)$$

where  $\theta$  is the angle between  $\vec{l}_{J^*}$  and  $\vec{Q}$ . Since  $Q^0 > |\vec{Q}|$  and  $Q^2 > 0$ , this factor is positive for small  $\vec{l}_{J^*}$  and negative for large  $\vec{l}_{J^*}$ . It thus vanishes for some  $\vec{l}_{J^*}$ , the value of which depends on  $\theta$ . We may call this a “scattering singularity” since it corresponds to on-shell 2 particle to  $n$  particle scattering. [An on-shell particle with momentum  $l_{J^*}^\mu$  scatters from an on-shell particle with momentum  $-l_{J^*+n}^\mu$  to make the final state particles. It is a simple exercise to show that  $-l_{J^*+n}^0 > 0$  in this case.] Note that this singularity is protected with an  $i\epsilon$  prescription.

We need to deform the contour in order to avoid the scattering singularities. However, we need to beware of the soft and collinear singularities that intersect the surface of a scattering singularity. There are two distinct cases to consider here.

First, the singular surface  $l_{J^*+2}^2 = 0$  includes the point at which  $l_{J^*+1}^\mu = 0$ . That is, the momentum transfer in this 2 particle to 2 particle scattering vanishes. This point is at the endpoint,  $x = 1$ , of the line  $l_{J^*}^\mu = xQ^\mu$  with  $0 < x < 1$ , where  $Q^\mu = l_{J^*}^\mu - l_{J^*+1}^\mu$ . On this line,  $l_{J^*}^\mu = (1-x)Q^\mu$ . The contour must not be deformed on this singular line. This is because the collinear singularity of this virtual graph cancels that of the real graph in which propagators  $J^*$  and  $J^* + 1$  are cut and we do not deform the contours for real graphs. For this reason, the deformation must vanish on the collinear line and must vanish on the scattering surface in the limit  $l_{J^*+1}^\mu \rightarrow 0$ . In fact, the deformation should vanish quadratically as we approach the point  $l_{J^*+1}^\mu = 0$ . That way, we maintain the necessary degree of cancellation between graphs with different cuts.

Similarly, the singular surface  $l_{J^*+n}^2 = 0$  for  $n > 2$  intersects the line  $l_{J^*}^\mu = xQ^\mu$  with  $1 < x < \infty$ , where again  $Q^\mu = l_{J^*}^\mu - l_{J^*+1}^\mu$ . This line does *not* represent a pinch singular surface for the virtual graph. However, it is the location of collinear singularities for the loopcuts in which propagators  $J^*$  and  $J^* + 1$  are cut. The collinear singularity cancels between these two loopcuts. Thus we can, and should, deform the contour along this line, so as to avoid the  $l_{J^*+n}^2 = 0$  singular surface. But we must be careful to keep the contour deformation the same along this line for both loopcuts.

We now examine the case of a virtual loop on the *right* hand side of the final state cut. In a typical term, one of the loop propagators, call it  $J^*$ , is “cut.” That is, we replace the propagator  $1/(l_{J^*}^2 - i\epsilon)$  by  $1/(2|\vec{l}_{J^*}|)$  and set  $l_{J^*}^0 = |\vec{l}_{J^*}|$  in the rest of the integrand. What kind of singularities does this give us for the other loop propagators? Let us examine each case in turn, taking into account the proper signs.

- $J = J^* + 1$ : We have  $l_{J^*+1}^\mu = l_{J^*}^\mu + Q^\mu$  where  $Q^2 = 0$  and  $Q^0 > 0$ . Thus

$$l_{J^*+1}^2 - i\epsilon = 2l_{J^*}^\mu Q_\mu - i\epsilon = 2|\vec{l}_{J^*}| |\vec{Q}| (1 - \cos \theta), \quad (193)$$

where  $\theta$  is the angle between  $\vec{l}_{J^*}$  and  $\vec{Q}$ . We thus have singularities when  $\vec{l}_{J^*}$  is soft and when it is collinear to  $\vec{Q}$ . Since these are endpoint singularities, there is no  $i\epsilon$  prescription for them.

- $J = J^* - 1$ : We have  $l_{J^*-1}^\mu = l_{J^*}^\mu - Q^\mu$  where  $Q^2 = 0$  and  $Q^0 > 0$ . Thus

$$l_{J^*-1}^2 - i\epsilon = -2l_{J^*}^\mu Q_\mu - i\epsilon = -2|\vec{l}_{J^*}| |\vec{Q}| (1 - \cos \theta), \quad (194)$$

where  $\theta$  is the angle between  $\vec{l}_{J^*}$  and  $\vec{Q}$ . We thus have singularities when  $\vec{l}_{J^*}$  is soft and when it is collinear to  $\vec{Q}$ . Again, there is no  $i\epsilon$  prescription.

- $J = J^* + n$  with  $n > 1$ : We have  $l_{J^*+n}^\mu = l_{J^*}^\mu + Q^\mu$  where  $Q^2 > 0$  and  $Q^0 > 0$ . Thus

$$l_{J^*-n}^2 - i\epsilon = 2l_{J^*}^\mu Q_\mu + Q^\mu Q_\mu - i\epsilon = 2|\vec{l}_{J^*}|(Q^0 - |\vec{Q}|\cos\theta) + Q^2, \quad (195)$$

where  $\theta$  is the angle between  $\vec{l}_{J^*}$  and  $\vec{Q}$ . Since  $Q^0 > |\vec{Q}|$  and  $Q^2 > 0$ , this factor is positive definite and does not give rise to a singularity.

- $J = J^* - n$  with  $n > 1$ : We have  $l_{J^*-n}^\mu = l_{J^*}^\mu - Q^\mu$  where  $Q^2 > 0$  and  $Q^0 > 0$ . Thus

$$l_{J^*-n}^2 - i\epsilon = -2l_{J^*}^\mu Q_\mu + Q^\mu Q_\mu - i\epsilon = -2|\vec{l}_{J^*}|(Q^0 - |\vec{Q}|\cos\theta) + Q^2 - i\epsilon, \quad (196)$$

where  $\theta$  is the angle between  $\vec{l}_{J^*}$  and  $\vec{Q}$ . Since  $Q^0 > |\vec{Q}|$  and  $Q^2 > 0$ , this factor is positive for small  $\vec{l}_{J^*}$  and negative for large  $\vec{l}_{J^*}$ . It thus vanishes for some  $\vec{l}_{J^*}$ , the value of which depends on  $\theta$ . Thus it exhibits a “scattering singularity,” which is protected with an  $i\epsilon$  prescription.

## 12 Some principles for choosing the deformation

Before beginning the discussion of the contour deformation, we state some of the key principles.

### 12.1 Singular surface

As discussed in Sec. 11, there is a singularity protected by an  $i\epsilon$  prescription when  $l^2 = 0$  and  $(l - Q)^2 = 0$  where  $Q^0 > 0$  and  $Q^2 > 0$ .

Let us consider, then, the generic case of the singular surface defined by  $l^2 = 0$  and  $(l - Q)^2 = 0$ , where  $E \equiv Q^0$  obeys  $E > |\vec{Q}|$ . The surface is the solution of

$$(|\vec{l}| - E)^2 = (\vec{l} - \vec{Q})^2. \quad (197)$$

That is

$$|\vec{l}| - E = \pm|\vec{l} - \vec{Q}|. \quad (198)$$

Since  $E > |\vec{Q}|$  the only possibility is

$$|\vec{l}| + |\vec{l} - \vec{Q}| = E. \quad (199)$$

This is an ellipsoid with its long axis in the direction of  $\vec{Q}$  and its center at  $\vec{l} = \vec{Q}/2$ .

The (not normalized) vector orthogonal to this surface is

$$\vec{w} = \frac{\vec{l}}{|\vec{l}|} + \frac{\vec{l} - \vec{Q}}{|\vec{l} - \vec{Q}|}. \quad (200)$$

## 12.2 Approximate direction of the deformation

The contour deformation will have the form  $\vec{l} \rightarrow \vec{l}_C$  where  $\vec{l}_C$  is complex and has the form

$$\vec{l}_C = \vec{l} - i C \vec{v}. \quad (201)$$

The vector  $\vec{v}$  gives the direction of deformation.

Consider the singular denominator  $(l - Q)^2 + i\epsilon$  when we take the loopcut that sets  $l^2 = 0$ . Then

$$(l_C - Q)^2 = (|\vec{l}_C| - E)^2 - (\vec{l}_C - \vec{Q})^2. \quad (202)$$

Expanding to first order in  $C$ , we find

$$(l_C - Q)^2 = (l - Q)^2 + 2i C \vec{v} \cdot \vec{A} + \dots, \quad (203)$$

where  $\vec{A} = E \vec{l}/|\vec{l}| - \vec{Q}$ . Evidently, when  $(l - Q)^2 = 0$ , the vector  $\vec{A}$  is in the direction of the normal to the surface specified by Eq. (197). That is,  $\vec{A}$  lies in the direction of the vector  $\vec{w}$ , Eq. (200). In order to make sure that the deformation keeps the pole of  $1/(l_C - Q)^2$  well away from the real axis, we would like to choose  $\vec{v}$  to be approximately in the direction of  $\vec{w}$  when  $(l - Q)^2 = 0$ .

## 12.3 Turning off the deformation near a pinch singularity

There is a cancellation among cuts at the collinear and soft singularities. Note that for the four-parton cuts, we do not want to deform the contours. (We want the momenta of final state particles to be real). For the three-parton cuts, we do want a deformation for the momentum in the virtual loop. In order to maintain the cancellation, then, we will need to insure that the deformation goes to zero at the pinch singularities.

The situation is a little more subtle. Consider the following toy integral,

$$I = \lim_{\delta \rightarrow 0} \int_\delta^1 \frac{dx}{x} \{f_1(x) - f_2(x)\}. \quad (204)$$

Here the endpoint singularity at  $x = 0$  plays the role of the pinch singularity and the two functions  $f_j$ , assumed analytic, play the role of the integrands for the three-parton and four-parton cuts, respectively. We suppose that

$$f_1(0) = f_2(0) \quad (205)$$

so that the apparent logarithmic divergence at  $x = 0$  is canceled.

Now we would like to deform the contour for the integration of  $f_1$ . We are tempted to choose the following two part contour that runs from 0 to 1 with a cutoff at  $\Re z = \delta$ :

$$\mathcal{C} : \left\{ \begin{array}{ll} z = \lambda e^{i\theta}, & \delta/\cos\theta < \lambda < 1 \\ z = e^{i\phi}, & \theta > \phi > 0 \end{array} \right\} \quad (206)$$

This would give the integral

$$I' = \lim_{\delta \rightarrow 0} \left\{ \int_{\mathcal{C}} \frac{dz}{z} f_1(z) - \int_{\delta}^1 \frac{dx}{x} f_1(x) \right\}. \quad (207)$$

We can write this as

$$I' = \lim_{\delta \rightarrow 0} \left\{ \int_{\mathcal{C}} \frac{dz}{z} f_1(z) - \int_{\delta}^1 \frac{dx}{x} f_1(x) \right\} + I. \quad (208)$$

Recognizing that  $(f_1(z) - f_1(0))/z$  is an analytic function and that the integral of an analytic function around a closed contour vanishes, we find

$$I' - I = f_1(0) \lim_{\delta \rightarrow 0} \left\{ \int_{\mathcal{C}} \frac{dz}{z} - \int_{\delta}^1 \frac{dx}{x} \right\}. \quad (209)$$

Performing the integral gives

$$I' - I = f_1(0) \{ \ln(\cos \theta) - i\theta \}. \quad (210)$$

The lesson here is that if we define the contour  $\mathcal{C}$  as  $z = x + iy(x)$ , then choosing  $y(x) \propto x$  for small  $x$  will give an integral  $I'$  that has a finite  $\delta \rightarrow 0$  limit but does not equal the original integral  $I$ . On the other hand, if  $y(x) \propto x^2$  for small  $x$ , we will get a finite  $I'$  with  $I' = I$ . That is, the deformed contour must approach the real axis quadratically as the distance to a pinch singularity goes to zero.

## 13 The deformation for a four propagator loop

Here we outline the functions for the deformation of a four propagator loop.

### 13.1 Notation

We consider here a loop to the left of the final state cut that has 4 propagators. One of the vertices in the loop is then the current vertex. The propagators in the loop are numbered  $J = 1, \dots, 4$  around the loop, starting at the current vertex. We let

$$\begin{aligned} \vec{l}_1 - \vec{l}_2 &= \vec{q}_3, \\ \vec{l}_2 - \vec{l}_3 &= \vec{q}_1, \\ \vec{l}_3 - \vec{l}_4 &= \vec{q}_2. \end{aligned} \quad (211)$$

Since  $\vec{l}_4 = \vec{l}_1$  in the reference frame we use, we have

$$\vec{q}_1 + \vec{q}_2 + \vec{q}_3 = 0. \quad (212)$$

## 13.2 Form of the deformation

To simplify the notation a little, we consider  $\vec{l}_1$  to be the independent variable and denote it simply by  $\vec{l}_1 = \vec{l}$ . Then  $\vec{l}_2 = \vec{l} - \vec{q}_1$ ,  $\vec{l}_3 = \vec{l} - \vec{q}_1 - \vec{q}_2$ , and  $\vec{l}_4 = \vec{l} - \vec{q}_1 - \vec{q}_2 - \vec{q}_3 = \vec{l}$ . (But  $l_4^0 = l_1^0 - \sqrt{s} \neq l_1^0$ .)

We are concerned with keeping the deformation zero near collinear singularities (to be discussed below) while having enough deformation to avoid the singularities associated with the two surfaces ( $l_1^2 = 0$  &  $l_3^2 = 0$ ) and ( $l_2^2 = 0$  &  $l_4^2 = 0$ ). There is another singular surface, ( $l_1^2 = 0$  &  $l_4^2 = 0$ ), but it lies further from the triangle and does not cause serious problems.

We are now prepared to specify the contour deformation precisely. We take complex loop momentum to have the form

$$l_C^i = l^i - i C(d^2) \left\{ F(\vec{l}) G_2(a_2) w_2^i(\vec{l}) + [1 - F(\vec{l})] G_3(a_3) w_3^i(\vec{l}) \right\}. \quad (213)$$

*Direction.* The direction of deformation is specified by two vectors  $\vec{w}_2$  and  $\vec{w}_3$ . We define these two vectors, along with a third, by

$$\begin{aligned} \vec{w}_2 &= \frac{\vec{l}_3}{|\vec{l}_3|} + \frac{\vec{l}_1}{|\vec{l}_1|}, \\ \vec{w}_3 &= \frac{\vec{l}_1}{|\vec{l}_1|} + \frac{\vec{l}_2}{|\vec{l}_2|}, \\ \vec{w}_1 &= \frac{\vec{l}_2}{|\vec{l}_2|} + \frac{\vec{l}_3}{|\vec{l}_3|}. \end{aligned} \quad (214)$$

Thus  $\vec{w}_2$  is the normal vector to a family of ellipsoids of which the surface ( $l_1^2 = 0$  &  $l_3^2 = 0$ ) is a member, while  $\vec{w}_3$  is the normal vector to a family of ellipsoids of which the surface ( $l_1^2 = 0$  &  $l_4^2 = 0$ ) is a member.

*Weighting factors.* The ellipsoid ( $l_1^2 = 0$  &  $l_3^2 = 0$ ) passes through the point  $\vec{l}_2 = 0$ , where there is a soft singularity. Near this point, we want the deformation to be precisely in the direction of  $\vec{w}_2$ . The ellipsoid ( $l_2^2 = 0$  &  $l_4^2 = 0$ ) passes through the point  $\vec{l}_3 = 0$ , where there is a soft singularity. Near this point, we want the deformation to be precisely in the direction of  $\vec{w}_3$ . For this reason we insert factors  $F$  and  $1 - F$  defined by

$$\begin{aligned} F(\vec{l}) &= \frac{\vec{l}_3^2}{\vec{l}_2^2 + \vec{l}_3^2}, \\ 1 - F(\vec{l}) &= \frac{\vec{l}_2^2}{\vec{l}_2^2 + \vec{l}_3^2}. \end{aligned} \quad (215)$$

*Turning off the deformation for large  $\vec{l}$ .* We define functions  $a_2(\vec{l})$  and  $a_3(\vec{l})$  by

$$\begin{aligned} a_2 &= |\vec{l}_3| + |\vec{l}_1| - |\vec{q}_2|, \\ a_3 &= |\vec{l}_1| + |\vec{l}_2| - |\vec{q}_3|. \end{aligned} \quad (216)$$

Also, we define parameters

$$\begin{aligned} A_2 &= |\vec{q}_3| + |\vec{q}_1| - |\vec{q}_2| = \sqrt{s} - 2|\vec{q}_2|, \\ A_3 &= |\vec{q}_1| + |\vec{q}_2| - |\vec{q}_3| = \sqrt{s} - 2|\vec{q}_3|. \end{aligned} \quad (217)$$

Surfaces of constant  $a_2$  are ellipsoids with foci at  $\vec{l}_3 = 0$  and  $\vec{l}_1 = 0$ . The surface ( $l_1^2 = 0$  &  $l_3^2 = 0$ ) is the surface  $a_2 = A_2$ . Similarly, surfaces of constant  $a_3$  are ellipsoids with foci at  $\vec{l}_1 = 0$  and  $\vec{l}_2 = 0$ . The surface ( $l_2^2 = 0$  &  $l_4^2 = 0$ ) is the surface  $a_3 = A_3$ .

We define functions  $G_n$  by

$$\begin{aligned} G_2(a_2) &= \frac{1}{A_2 + \gamma a_2}, \\ G_3(a_3) &= \frac{1}{A_3 + \gamma a_3}. \end{aligned} \quad (218)$$

Here  $\gamma$  is an adjustable parameter. The purpose of the functions  $G_n$  is to turn the deformation off when  $\vec{l}$  gets beyond the critical ellipsoids.

*Turning off the deformation near the collinear singularities.* Define

$$\begin{aligned} d_2 &= |\vec{l}_3| |\vec{l}_1| |\vec{w}_2| / |\vec{q}_2|, \\ d_3 &= |\vec{l}_1| |\vec{l}_2| |\vec{w}_3| / |\vec{q}_3|, \\ d_1 &= |\vec{l}_2| |\vec{l}_3| |\vec{w}_1| / |\vec{q}_1|. \end{aligned} \quad (219)$$

The function  $d_2$  vanishes along the line  $\vec{l}_3 = \lambda \vec{q}_2$ ,  $0 < \lambda < 1$ . The amplitude has a collinear singularity along this line. This collinear singularity cancels between the real and virtual graphs. Thus we do not want to deform the contour for the virtual graph when  $\vec{l}_3$  lies on this line. For this reason, we will insure that the deformation vanishes for  $d_2 \rightarrow 0$ . The other two functions  $d_J$  vanish on the other two collinear singularities, so we will in fact insure that the deformation vanishes when any of the  $d_J$  approaches 0. To this end, we define

$$d = \min(d_1, d_2, d_3). \quad (220)$$

Then we include in Eq. (213) a factor

$$C(d^2) = \frac{\alpha \eta d^2}{1 + \beta d^2/\Lambda_C^2}. \quad (221)$$

where

$$\Lambda_C^2 = s/4. \quad (222)$$

Here  $\alpha$  and  $\beta$  are adjustable parameters.

*Sign.* We include in  $C$  a factor  $\eta$ , which is +1 for a loop to the left of the cut, -1 for a loop to the right of the cut.

### 13.3 The jacobian

The jacobian for the contour deformation is

$$\mathcal{J} = \det A \quad (223)$$

where

$$A^{ij} = \frac{\partial l_C^i}{\partial l^j}. \quad (224)$$

We thus need the gradients of the various functions that enter Eq. (213). We adopt the notation that  $J \pm 1$  means  $[J \pm 1]_{\text{mod } 3}$ . Then we find

$$\frac{\partial w_J^i}{\partial l^j} = \frac{1}{|\vec{l}_{J+1}|} \left( \delta^{ij} - \frac{l_{J+1}^i l_{J+1}^j}{\vec{l}_{J+1}^2} \right) + \frac{1}{|\vec{l}_{J-1}|} \left( \delta^{ij} - \frac{l_{J-1}^i l_{J-1}^j}{\vec{l}_{J-1}^2} \right), \quad (225)$$

$$\frac{\partial a_J}{\partial l^j} = w_J^j, \quad (226)$$

$$\frac{\partial d_J^2}{\partial l^j} = 2d_J^2 \left( \frac{l_{J+1}^j}{\vec{l}_{J+1}^2} + \frac{l_{J-1}^j}{\vec{l}_{J-1}^2} + \frac{1}{\vec{w}_J^2} w_J^i \frac{\partial w_J^i}{\partial l^j} \right), \quad (227)$$

$$\frac{\partial F}{\partial l^j} = \frac{2}{(\vec{l}_2^2 + \vec{l}_3^2)^2} (\vec{l}_2^2 l_3^j - \vec{l}_3^2 l_2^j). \quad (228)$$

We also need

$$\frac{1}{G_J(a_J)} \frac{dG_J(a_J)}{da_J} = -\frac{\gamma}{A_J + \gamma a_J}, \quad (229)$$

$$\frac{1}{C(d^2)} \frac{dC(d^2)}{dd^2} = \frac{1}{d^2 (1 + \beta d^2 / \Lambda_C^2)}. \quad (230)$$

The derivative matrix  $A^{ij}$  can be written in terms of these gradients as

$$\begin{aligned} A^{ij} &= \delta^{ij} \\ &- iC \left\{ \frac{1}{C} \frac{\partial C}{\partial d^2} \frac{\partial d^2}{\partial l^j} (F G_2 w_2^i + [1 - F] G_3 w_3^i) \right. \\ &\quad + \frac{\partial F}{\partial l^j} (G_2 w_2^i - G_3 w_3^i) \\ &\quad + F \frac{\partial G_2}{\partial a_2} w_2^i w_2^j + [1 - F] \frac{\partial G_3}{\partial a_3} w_3^i w_3^j \\ &\quad \left. + F G_2 \frac{\partial w_2^i}{\partial l^j} + [1 - F] G_3 \frac{\partial w_3^i}{\partial l^j} \right\} \end{aligned} \quad (231)$$

## 14 The deformation for a three propagator loop that connects to the current vertex

We consider a three point virtual subgraph like that shown in the figure. One of the vertices connects to the current vertex. One of the vertices connects to a propagator that enters the final state. The third connects to a virtual propagator that connects to two propagators that enter the final state. The propagators in the loop are numbered  $J = 1, \dots, 3$  around the loop, starting at the current vertex. It is helpful to take the next vertex to be the one that connects to a cut propagator. However, the final formulas will work independently of which way we go around the loop. We adopt the notation

$$\begin{aligned}\vec{l}_1 - \vec{l}_2 &= \vec{q}_3, \\ \vec{l}_2 - \vec{l}_3 &= \vec{q}_1.\end{aligned}\tag{232}$$

We will be concerned with deforming around the singularity ( $l_2^2 = 0$  &  $l_3^2 = 0$ ). Accordingly we define

$$l_C^i = l^i - i C(d^2) G_3(a_3) w_3^i(\vec{l}).\tag{233}$$

*Direction.* The direction of deformation is specified by the vector  $\vec{w}_3$ , defined by

$$\vec{w}_3 = \frac{\vec{l}_1}{|\vec{l}_1|} + \frac{\vec{l}_2}{|\vec{l}_2|}.\tag{234}$$

Thus  $\vec{w}_3$  is the normal vector to a family of ellipsoids of which the surface ( $l_2^2 = 0$  &  $l_3^2 = 0$ ) is a member.

*Turning off the deformation for large  $\vec{l}$ .* We define a function  $a(\vec{l})$  by

$$a_3 = |\vec{l}_1| + |\vec{l}_2| - |\vec{q}_3|.\tag{235}$$

Also, we define a parameter

$$A_3 = \sqrt{s} - 2|\vec{q}_3|.\tag{236}$$

Surfaces of constant  $a$  are ellipsoids with foci at  $\vec{l}_1 = 0$  and  $\vec{l}_2 = 0$ . The surface ( $l_1^2 = 0$  &  $l_3^2 = 0$ ) is the surface  $a_3 = A_3$ .

We define the function  $G_3$  by

$$G_3(a_3) = \frac{1}{A_3 + \gamma a_3}.\tag{237}$$

The purpose of the function  $G_3$  is to turn the deformation off when  $\vec{l}$  gets beyond the critical ellipsoid.

*Turning off the deformation near the collinear singularities.* Define

$$d = d_3 = |\vec{l}_1| |\vec{l}_2| |\vec{w}_3| / |\vec{q}_3|.\tag{238}$$

The function  $d$  vanishes along the line  $\vec{l}_1 = \lambda \vec{q}_3$ ,  $0 < \lambda < 1$ . The amplitude has a collinear singularity along this line. This collinear singularity cancels between the real and virtual graphs. Thus we do not want to deform the contour for the virtual graph when  $\vec{l}_1$  lies on this line. For this reason, we include in Eq. (233) a factor [*This  $\beta$  is DFRM2. Check on consistency of the names for the various  $\beta$ s.*]

$$C(d^2) = \frac{\alpha \eta d^2}{1 + \beta d^2/\Lambda_C^2}, \quad (239)$$

where

$$\Lambda_C^2 = |\vec{q}_3|^2. \quad (240)$$

*Sign.* We include in  $C$  a factor  $\eta$ , which is  $+1$  for a loop to the left of the cut,  $-1$  for a loop to the right of the cut.

## 14.1 The jacobian

The jacobian for the contour deformation is again  $\mathcal{J} = \det A$  where  $A^{ij} = \partial l_C^i / \partial l^j$ . We thus need the gradients of the various functions that enter Eq. (233). We use the formulas in Sec. 13.3.

The derivative matrix  $A^{ij}$  can be written in terms of these gradients as

$$A^{ij} = \delta^{ij} - iC G \left\{ \frac{1}{C} \frac{\partial C}{\partial d^2} \frac{\partial d^2}{\partial l^j} w_3^i + \frac{1}{G_3} \frac{\partial G_3}{\partial a_3} w_3^i w_3^j + \frac{\partial w_3^i}{\partial l^j} \right\}. \quad (241)$$

## 15 The deformation for a three propagator loop that does not connect to the current vertex

Here we outline the functions for the deformation of a three propagator loop that does not connect to the current vertex.

### 15.1 Notation

We consider here a loop to the left of the final state cut that has three vertices, two of which connect to propagators that enter the final state. The remaining vertex then connects to a propagator that connects to the current vertex. The propagators in the loop are numbered  $J = 1, \dots, 3$  around the loop, starting at the vertex that does not connect to a cut propagator. We let

$$\begin{aligned} \vec{l}_1 - \vec{l}_2 &= \vec{q}_3, \\ \vec{l}_2 - \vec{l}_3 &= \vec{q}_1, \\ \vec{l}_3 - \vec{l}_1 &= \vec{q}_2. \end{aligned} \quad (242)$$

## 15.2 Form of the deformation

We consider  $\vec{l}_1$  to be the independent variable and denote it simply by  $\vec{l}_1 = \vec{l}$ .

We are concerned with keeping the deformation zero near collinear singularities while having enough deformation to avoid the singularities associated with the surface ( $l_1^2 = 0$  &  $l_3^2 = 0$ ).

We are now prepared to specify the contour deformation precisely. We take complex loop momentum to have the form

$$l_C^i = l^i - i C(d^2) G_2(a_2) w_2^i(\vec{l}). \quad (243)$$

*Direction.* The direction of deformation is specified by the vectors  $\vec{w}_2$ . We define three vector  $\vec{w}_J$  by

$$\begin{aligned} \vec{w}_2 &= \frac{\vec{l}_3}{|\vec{l}_3|} + \frac{\vec{l}_1}{|\vec{l}_1|}, \\ \vec{w}_3 &= \frac{\vec{l}_1}{|\vec{l}_1|} + \frac{\vec{l}_2}{|\vec{l}_2|}, \\ \vec{w}_1 &= \frac{\vec{l}_2}{|\vec{l}_2|} + \frac{\vec{l}_3}{|\vec{l}_3|}. \end{aligned} \quad (244)$$

Thus  $\vec{w}_2$  is the normal vector to a family of ellipsoids of which the surface ( $l_1^2 = 0$  &  $l_3^2 = 0$ ) is a member.

*Turning off the deformation for large  $\vec{l}$ .* We define function  $a_2(\vec{l})$  by

$$a_2 = |\vec{l}_3| + |\vec{l}_1| - |\vec{q}_2|. \quad (245)$$

Also, we define the parameter

$$A_2 = |\vec{q}_3| + |\vec{q}_1| - |\vec{q}_2| = \sqrt{s} - 2|\vec{q}_2|. \quad (246)$$

Surfaces of constant  $a_2$  are ellipsoids with foci at  $\vec{l}_3 = 0$  and  $\vec{l}_1 = 0$ . The surface ( $l_1^2 = 0$  &  $l_3^2 = 0$ ) is the surface  $a_2 = A_2$ .

We define a function  $G_2$  by

$$G_2(a_2) = \frac{1}{A_2 + \gamma a_2}. \quad (247)$$

Here  $\gamma$  is an adjustable parameter. The purpose of the function  $G_2$  is to turn the deformation off when  $\vec{l}$  gets beyond the critical ellipsoid.

*Turning off the deformation near the collinear singularities.* Define

$$\begin{aligned} d_3 &= |\vec{l}_1| |\vec{l}_2| |\vec{w}_3| / |\vec{q}_3|, \\ d_1 &= |\vec{l}_2| |\vec{l}_3| |\vec{w}_1| / |\vec{q}_1|. \end{aligned} \quad (248)$$

The function  $d_3$  vanishes along the line  $\vec{l}_1 = \lambda \vec{q}_3$ ,  $0 < \lambda < 1$ . The amplitude has a collinear singularity along this line. The function  $d_1$  vanishes along the line  $\vec{l}_2 = \lambda \vec{q}_1$ ,  $0 < \lambda < 1$ . The amplitude has a collinear singularity along this line also. In order to insure that the deformation vanishes at these two collinear singularities, we define

$$d = \min(d_1, d_3). \quad (249)$$

Then we include in Eq. (243) a factor

$$C(d^2) = \frac{\alpha \eta d^2}{1 + \beta d^2/\Lambda_C^2}, \quad (250)$$

where

$$\Lambda_C^2 = s/4. \quad (251)$$

*Sign.* We include a factor  $\eta$ , which is  $+1$  for a loop to the left of the cut,  $-1$  for a loop to the right of the cut.

### 15.3 The jacobian

The jacobian for the contour deformation is again  $\mathcal{J} = \det A$  where  $A^{ij} = \partial l_C^i / \partial l^j$ . We thus need the gradients of the various functions that enter Eq. (243). We use the formulas in Sec. 13.3.

The derivative matrix  $A^{ij}$  can be written in terms of these gradients as

$$A^{ij} = \delta^{ij} - iC G_2 \left\{ \frac{1}{C} \frac{\partial C}{\partial d^2} \frac{\partial d^2}{\partial l^j} w_2^i + \frac{1}{G_2} \frac{\partial G_2}{\partial a_2} w_2^i w_2^j + \frac{\partial w_2^i}{\partial l^j} \right\}. \quad (252)$$

## 16 The deformation for a two propagator loop

Here we outline the functions for the deformation of a two propagator loop.

### 16.1 Notation

We consider here a loop to the left of the final state cut that has two propagators. One of the vertices connects to a propagator all of whose momentum enters the final state. There are two possible cases: either this propagator itself enters the final state or it connects to two propagators that do enter the final state. In the first case, no deformation is needed. Thus we discuss the second case. However, we will apply the same formulas for the first case also.

The propagators in the loop are numbered  $J = 1, 2$  around the loop, starting at vertex that does not connect to a final state propagator. We let

$$\vec{l}_1 - \vec{l}_2 = \vec{q}_3. \quad (253)$$

## 16.2 Form of the deformation

We consider  $\vec{l}_1$  to be the independent variable and denote it simply by  $\vec{l}_1 = \vec{l}$ .

We are concerned with keeping the deformation zero near collinear singularities while having enough deformation to avoid the singularities associated with the surface ( $l_1^2 = 0$  &  $l_2^2 = 0$ ).

We are now prepared to specify the contour deformation precisely. We take complex loop momentum to have the form

$$l_C^i = l^i - i C(d^2) G_3(a_3) w_3^i(\vec{l}). \quad (254)$$

*Direction.* The direction of deformation is specified by the vectors  $\vec{w}_3$ , by

$$\vec{w}_3 = \frac{\vec{l}_1}{|\vec{l}_1|} + \frac{\vec{l}_2}{|\vec{l}_2|}. \quad (255)$$

Thus  $\vec{w}_3$  is the normal vector to a family of ellipsoids of which the surface ( $l_1^2 = 0$  &  $l_2^2 = 0$ ) is a member.

*Turning off the deformation for large  $\vec{l}$ .* We define function  $a_2(\vec{l})$  by

$$a_3 = |\vec{l}_1| + |\vec{l}_2| - |\vec{q}_3|. \quad (256)$$

Also, we define the parameter

$$A_3 = \sqrt{s} - 2|\vec{q}_3|. \quad (257)$$

Surfaces of constant  $a_3$  are ellipsoids with foci at  $\vec{l}_1 = 0$  and  $\vec{l}_2 = 0$ . The surface ( $l_1^2 = 0$  &  $l_2^2 = 0$ ) is the surface  $a_3 = A_3$ .

We define a function  $G_3$  by

$$G_3(a_3) = \frac{1}{A_3 + \gamma a_3}. \quad (258)$$

Here  $\gamma$  is an adjustable parameter. The purpose of the function  $G_3$  is to turn the deformation off when  $\vec{l}$  gets beyond the critical ellipsoid.

*Turning off the deformation near the collinear singularities.* Define

$$d = d_3 = |\vec{l}_1| |\vec{l}_2| |\vec{w}_3| / |\vec{q}_3|. \quad (259)$$

The function  $d_3$  vanishes along the line  $\vec{l}_1 = \lambda \vec{q}_3$ ,  $0 < \lambda < 1$ . The amplitude does not have a collinear singularity along this line in the case that the propagator attached to the virtual loop is not cut, but in the case that this propagator is cut, there is a collinear singularity along this line. Since we deal with these cases together, we insure that the deformation vanishes along this line by including in Eq. (254) a factor

$$C(d^2) = \frac{\alpha \eta d^2}{1 + \beta d^2/\Lambda_C^2} \frac{A_3}{\sqrt{s}}, \quad (260)$$

where

$$\Lambda_C^2 = |\vec{q}_3|^2. \quad (261)$$

The factor  $A_3/\sqrt{s}$  here turns the deformation off as the momentum  $q_3^\mu$  entering the self energy becomes nearly lightlike.

*Sign.* We include in  $C$  a factor  $\eta$ , which is +1 for a loop to the left of the cut, -1 for a loop to the right of the cut.

### 16.3 The jacobian

The jacobian for the contour deformation is again  $\mathcal{J} = \det A$  where  $A^{ij} = \partial l_C^i / \partial l^j$ . We thus need the gradients of the various functions that enter Eq. (243). We use the formulas in Sec. 13.3.

The derivative matrix  $A^{ij}$  can be written in terms of these gradients as

$$A^{ij} = \delta^{ij} - iC G_3 \left\{ \frac{1}{C} \frac{\partial C}{\partial d^2} \frac{\partial d^2}{\partial l^j} w_3^i + \frac{1}{G_3} \frac{\partial G_3}{\partial a_3} w_3^i w_3^j + \frac{\partial w_3^i}{\partial l^j} \right\}. \quad (262)$$

## 17 Renormalization of three point functions

In this section, we consider how to renormalize the divergent one loop virtual three point functions using numerical integration. We will discuss two point functions in a subsequent section.

### 17.1 Quark-antiquark-boson vertices

In this subsection, we first study the quark-antiquark-gluon vertex. Then we extend the result to the quark-antiquark-photon vertex, which has essentially the same structure.

There are two contributions to the quark-antiquark-gluon vertex  $\Gamma_a^\mu(k_1, k_2)$  at one loop. Each of them has the form

$$\Gamma_a^\mu(k_1, k_2) = ig^2 C t_a \tilde{\mu}^{2\epsilon} \int \frac{d^{4-2\epsilon} l}{(2\pi)^{4-2\epsilon}} \frac{N^\mu(l, k_1, k_2)}{[(k_2 - l)^2 + i\epsilon][(k_1 - l)^2 + i\epsilon][l^2 + i\epsilon]}, \quad (263)$$

where  $C$  is the color factor for that graph. The numerator function has the form

$$N^\mu = A_1(\epsilon) l^\mu + A_2(\epsilon) l^2 \gamma^\mu + \mathcal{O}(l). \quad (264)$$

Here the omitted terms have one or zero powers of  $l$  and, correspondingly, one or two powers of  $k_1$  or  $k_2$ .

We subtract a suitably chosen quantity  $\tilde{\Gamma}_a^\mu$  from  $\Gamma_a^\mu(k_1, k_2)$ :

$$\tilde{\Gamma}_a^\mu = ig^2 C t_a \tilde{\mu}^{2\epsilon} \int \frac{d^{4-2\epsilon} l}{(2\pi)^{4-2\epsilon}} \frac{\tilde{N}(l)^\mu}{D(l^2)^3}, \quad (265)$$

where  $D(l^2) = l^2 - M^2 + i\epsilon$ . The numerator function here is

$$\tilde{N}(l^\mu) = A_1(\epsilon) l^\mu + A_2(\epsilon) l^2 \gamma^\mu + M^2 B_1(\epsilon) \gamma^\mu, \quad (266)$$

where

$$B_1(\epsilon) = \frac{1}{2} \frac{A_1(\epsilon) - A_1(0)}{\epsilon} + 2 \frac{A_2(\epsilon) - A_2(0)}{\epsilon} - A_2(\epsilon). \quad (267)$$

Two properties of  $\tilde{\Gamma}_a^\mu$  are important. First, the integrand of  $\tilde{\Gamma}_a^\mu$  matches that of  $\Gamma_a^\mu$  for large  $l^\mu$  up to terms of order  $l^{-6}$ . Second, it is easy to compute  $\tilde{\Gamma}_a^\mu$ , with the result

$$\tilde{\Gamma}_a^\mu = -\frac{\alpha_s}{4\pi} C t_a X_1 \gamma^\mu \Gamma(\epsilon) \left( \frac{4\pi\tilde{\mu}^2}{M^2} \right)^\epsilon. \quad (268)$$

where

$$X_1 = \frac{1}{4} A_1(0) + A_2(0). \quad (269)$$

Without the  $B_1(\epsilon)$  term in  $\tilde{\Gamma}_a^\mu$ , the coefficient  $X_1$  would be  $\epsilon$  dependent, which would affect the finite part of the result as  $\epsilon \rightarrow 0$ .

Expanding Eq. (268) about  $\epsilon = 0$ , we have

$$\tilde{\Gamma}_a^\mu = [\tilde{\Gamma}_a^\mu]_{\text{pole}} + [\tilde{\Gamma}_a^\mu]_{\text{R}} + \mathcal{O}(\epsilon), \quad (270)$$

with

$$\begin{aligned} [\tilde{\Gamma}_a^\mu]_{\text{pole}} &= -\frac{\alpha_s}{4\pi} C t_a X_1 \gamma^\mu \frac{1}{\epsilon}, \\ [\tilde{\Gamma}_a^\mu]_{\text{R}} &= -\frac{\alpha_s}{4\pi} C t_a X_1 \gamma^\mu \ln\left(\frac{\mu^2}{M^2}\right). \end{aligned} \quad (271)$$

We can use our results for  $\tilde{\Gamma}_a^\mu$  to write

$$[\Gamma_a^\mu]_{\text{R}} = \left\{ \Gamma_a^\mu - \tilde{\Gamma}_a^\mu \right\}_{\epsilon=0} + [\tilde{\Gamma}_a^\mu]_{\text{R}}. \quad (272)$$

The first term can be evaluated by numerical integration in 4 dimensions. The second term vanishes if we set

$$M^2 = \mu^2. \quad (273)$$

Now, what we need for calculational purposes are the coefficients in  $\tilde{N}$ , Eqs. (265) and (266) evaluated at  $\epsilon = 0$ . For the graph in which the gluon connects to the gluon line, one finds

$$C = N_c/2, \quad A_1(\epsilon) = -4(1-\epsilon), \quad A_2(\epsilon) = -2, \quad B_1(0) = 4. \quad (274)$$

For the graph in which the gluon connects to the quark line, one finds

$$C = -1/[2N_c], \quad A_1(\epsilon) = 4(1-\epsilon), \quad A_2(\epsilon) = -2(1-\epsilon), \quad B_1(0) = 4. \quad (275)$$

If we change  $C$  from  $-1/[2N_c]$  to  $C_F = (N_c^2 - 1)/[2N_c]$ , this same result holds for the quark-antiquark-photon vertex, with the appropriate change in the color structure from  $C t_a$  to  $C$ .

## 17.2 Performing the energy integrations

We have learned how to renormalize the virtual three point functions that we encounter in a fashion that works in four dimensions but is equivalent to  $\overline{\text{MS}}$  renormalization. Here, we deal with the implementation of the loop integrals as numerical integrals.

In our virtual one-loop graphs, we perform the integrations over the loop energy analytically. As described in Sec. 1.2, this is easy for a typical graph with non-zero incoming momenta. However, the counter terms for the UV divergent graphs need a special treatment. Here, we have singular factors of the form

$$\frac{1}{D(l^2)^N} \equiv \frac{1}{(l^2 - M^2 + i\epsilon)^N} = \frac{1}{(l^0 - \omega + i\epsilon)^N} \frac{1}{(l^0 + \omega - i\epsilon)^N} \quad (276)$$

where

$$\omega = \sqrt{\vec{l}^2 + M^2}. \quad (277)$$

To perform an integral

$$I = i \int \frac{dl^0}{2\pi} \frac{f(l^0)}{D(l^2)^N} \quad (278)$$

we close the integration contour in the lower half plane and find

$$I = \left[ \frac{1}{(N-1)!} \left( \frac{d}{dl^0} \right)^{N-1} \frac{f(l^0)}{(l^0 + \omega)^N} \right]_{l^0=\omega}. \quad (279)$$

We present the results below.

For a quark-antiquark-gluon vertex, we need  $\tilde{\Gamma}_a^\mu$ , which we write in the form

$$\tilde{\Gamma}_a^\mu = g^2 C t_a \int \frac{d\vec{l}}{(2\pi)^3} I(\vec{l})^\mu. \quad (280)$$

The form for a quark-antiquark-photon vertex is the same without the  $t_a$ . Here

$$I(\vec{l})^\mu = i \int \frac{dl^0}{2\pi} \frac{\tilde{N}(l)^\mu}{D(l^2)^3}, \quad (281)$$

where

$$\tilde{N}^\mu = A_1(0) \not{l}^\mu + A_2(0) l^2 \gamma^\mu + M^2 B_1(0) \gamma^\mu. \quad (282)$$

Performing the integration gives

$$I^\mu = \frac{-A_1(0)\gamma^0 n^\mu - 4A_2(0)\gamma^\mu}{16\omega^3} + \frac{3A_1(0)\tilde{l}\tilde{l}^\mu + 3(A_2(0) + B_1(0))M^2\gamma^\mu}{16\omega^5}. \quad (283)$$

Here, as before,  $n^\mu = (1, \vec{0})$ . I denote the four vector containing only the space-components of  $l^\mu$  by  $\tilde{l}^\mu$ . Thus  $\tilde{l}^\mu = (0, \vec{l})$ . The coefficients  $A_n$  and  $B_1$  can be found in Eqs. (274) and (275).

## 18 Gluon self-energy

In this section, we consider the gluon self-energy graphs, including their renormalization.

### 18.1 Coulomb gauge projection

Consider a one-loop gluon self-energy graph in Feynman gauge,

$$\pi(q)_{F ab}^{\mu\nu} = ig^2 \delta_{ab} \tilde{q}^{2\epsilon} \int \frac{d^{4-2\epsilon}l}{(2\pi)^{4-2\epsilon}} \frac{N(l; q)_F^{\mu\nu}}{[(l - \frac{1}{2}q)^2 + i\epsilon][(l + \frac{1}{2}q)^2 + i\epsilon]}, \quad (284)$$

Our calculation will contain such graphs along with the corresponding cut graphs

$$\Pi(q)_{F ab}^{\mu\nu} = ig^2 \delta_{ab} \int \frac{d^4 l}{(2\pi)^2} N(l; q)_F^{\mu\nu} \delta_+((l - \frac{1}{2}q)^2) \delta_+((l + \frac{1}{2}q)^2). \quad (285)$$

(For the cut graph, the measurement function  $\mathcal{S}$  and the smearing function  $h(\sqrt{s})$  depend on  $l^\mu$ , although we do not indicate this dependence explicitly above.)

In either of these functions, terms proportional to  $q^\mu q^\nu$  would cause problems in our numerical approach. Therefore, we multiply on the left and on the right by

$$P(q)_\alpha^\mu = g_\alpha^\mu - \frac{q^\mu \tilde{q}_\alpha}{\tilde{q}^2} \quad (286)$$

where

$$\tilde{q} = (0, \vec{q}). \quad (287)$$

This gives us

$$\pi(q)_{ab}^{\mu\nu} = P(q)_\alpha^\mu \pi(q)_{Fab}^{\alpha\beta} P(q)_\beta^\nu. \quad (288)$$

We are allowed to do this because the  $q^\mu$  and  $q^\nu$  terms will give zero contributions after we sum over graphs. We make the same projection for the cut self-energy graphs.

The self energy in Feynman gauge has the structure

$$\pi(q)_{F ab}^{\mu\nu} = (g^{\mu\nu} q^2 - q^\mu q^\nu) \delta_{ab} \pi(q^2) \quad (289)$$

After multiplying by the matrices  $P$ , the  $q^\mu$  terms do not contribute, since

$$P(q)_\alpha^\mu q^\alpha = 0. \quad (290)$$

This leaves

$$\pi(q)_{ab}^{\mu\nu} = T(q)^{\mu\nu} \delta_{ab} q^2 \pi(q^2), \quad (291)$$

where

$$T(q)^{\mu\nu} = g^{\mu\nu} - \frac{1}{\tilde{q}^2} (q^\mu \tilde{q}^\nu + \tilde{q}^\mu q^\nu - q^\mu q^\nu). \quad (292)$$

Note that

$$T(q)^{ij} = -\left(\delta_{ij} - \frac{q^i q^j}{\vec{q}^2}\right), \quad T(q)^{i0} = T(q)^{0j} = 0, \quad T(q)^{00} = -\frac{q^2}{\vec{q}^2}. \quad (293)$$

We will be interested in  $\pi(q)^{\mu\nu}/q^2$  evaluated at  $q^2 = 0$  (with  $\vec{q} \neq 0$ ). We see that this tensor does have a finite  $q^2 \rightarrow 0$  limit, and that the  $0i$  and  $00$  components of the limiting tensor are zero. Thus we need consider only  $\pi(q)^{ij}/q^2$  at  $q^2 = 0$ .

## 18.2 Structure of the gluon self-energy

Consider the one loop gluon self-energy, summed over the contributions from a quark loop, a gluon loop, and a ghost loop. The self-energy, including the Coulomb gauge projection, has the form

$$\pi(q)_{ab}^{\mu\nu} = ig^2 \delta_{ab} \tilde{\mu}^{2\epsilon} \int \frac{d^{4-2\epsilon}l}{(2\pi)^{4-2\epsilon}} \frac{N(l; q)^{\mu\nu}}{[(l - \frac{1}{2}q)^2 + i\epsilon][(l + \frac{1}{2}q)^2 + i\epsilon]}, \quad (294)$$

where the scale factor  $\tilde{\mu}$  is related to the  $\overline{\text{MS}}$  scale factor  $\mu$  by  $\mu^2 = 4\pi\tilde{\mu}^2 e^{-\gamma}$ , where  $\gamma = 0.577\cdots$  is Euler's constant. The numerator function is defined by

$$N(l; q)^{\mu\nu} = P(q)_\alpha^\mu N(l; q)_{F ab}^{\alpha\beta} P(q)_\beta^\nu, \quad (295)$$

where

$$N_F^{\mu\nu} = A_1(\epsilon) l^\mu l^\nu + A_2(\epsilon) g^{\mu\nu} l^2 + A_3(\epsilon) q^\mu q^\nu + A_4(\epsilon) g^{\mu\nu} q^2. \quad (296)$$

(There is also a term proportional to  $q^\mu l^\nu - l^\mu q^\nu$ , which will drop out of our calculation.) The coefficients  $A_i(\epsilon)$  are polynomials in  $\epsilon$ . The specific contributions are as follows, where the prefactors are the color factors ( $N_f$  = number of flavors):

$$\begin{aligned} \text{Gluon loop} \quad (A_1, A_2, A_3, A_4) &= N_c \times (5 - 4\epsilon, 1, -9/4, 9/4) \\ \text{Ghost loop} \quad (A_1, A_2, A_3, A_4) &= N_c \times (-1, 0, 1/4, 0) \\ \text{Quark loop} \quad (A_1, A_2, A_3, A_4) &= (N_f/2) \times (-8, 4, 2, -1) \end{aligned} \quad (297)$$

Thus

$$A_1(\epsilon) = 4N_c - 4N_f - 4N_c\epsilon \quad A_2(\epsilon) = N_c + 2N_f \quad A_3(\epsilon) = -2N_c + N_f \quad A_4(\epsilon) = \frac{9N_c}{4} - \frac{N_f}{2}. \quad (298)$$

After the Coulomb gauge projection, we have

$$N^{\mu\nu} = A_1(\epsilon) l_P^\mu l_P^\nu + A_2(\epsilon) T(q)^{\mu\nu} l^2 + A_4(\epsilon) T(q)^{\mu\nu} q^2. \quad (299)$$

Here

$$l_P^\mu = l^\mu - q^\mu \frac{\vec{q} \cdot \vec{l}}{\vec{q}^2} \quad (300)$$

and  $T(q)^{\mu\nu}$  is defined in Eq. (292).

### 18.3 Dispersive representation

We need to calculate  $\pi(q)_{ab}^{\mu\nu}/q^2$  at  $q^2 = 0$ . The discussion after Eq. (291) tells us that we need only consider the space components of this tensor.

Thus we consider  $f(E) \equiv \pi(E, \vec{q})_{ab}^{ij}/(E^2 - \vec{q}^2)$ . This function is analytic in the  $E$  plane cut along the real axis from  $-\infty$  to  $-|\vec{q}|$  and from  $|\vec{q}|$  to  $\infty$ . Thus

$$f(E) = \frac{1}{2\pi i} \int_{|\vec{q}|}^{\infty} d\bar{E} \left\{ \frac{\text{disc}f(\bar{E})}{\bar{E} - E} - \frac{\text{disc}f(-\bar{E})}{\bar{E} + E} \right\}. \quad (301)$$

We find for the discontinuity of  $f(E)$  for positive  $E$

$$\begin{aligned} \text{disc}f(\bar{E}) &= -ig^2 \delta_{ab} \tilde{\mu}^{2\epsilon} \int \frac{d^{3-2\epsilon} \vec{l}}{(2\pi)^{3-2\epsilon}} (2\pi) \delta(|\vec{k}_+| + |\vec{k}_-| - \bar{E}) \\ &\times \frac{N\left(\frac{1}{2}(|\vec{k}_+| - |\vec{k}_-|), \vec{l}; |\vec{k}_+| + |\vec{k}_-|, \vec{q}\right)^{ij}}{2|\vec{k}_+| 2|\vec{k}_-| (\bar{E}^2 - \vec{q}^2)} \end{aligned} \quad (302)$$

Here we have denoted

$$\vec{k}_{\pm} = \frac{1}{2}\vec{q} \pm \vec{l}. \quad (303)$$

For negative  $E$  we find

$$\begin{aligned} \text{disc}f(-\bar{E}) &= ig^2 \delta_{ab} \tilde{\mu}^{2\epsilon} \int \frac{d^{3-2\epsilon} \vec{l}}{(2\pi)^{3-2\epsilon}} (2\pi) \delta(|\vec{k}_+| + |\vec{k}_-| - \bar{E}) \\ &\times \frac{N\left(-\frac{1}{2}(|\vec{k}_+| - |\vec{k}_-|), \vec{l}; -|\vec{k}_+| - |\vec{k}_-|, \vec{q}\right)^{ij}}{2|\vec{k}_+| 2|\vec{k}_-| (\bar{E}^2 - \vec{q}^2)} \end{aligned} \quad (304)$$

We insert these results into Eq. (301), and use the fact that the numerator function is an even function of the energies:

$$N(-l^0, \vec{l}; -q^0, \vec{q})^{ij} = N(l^0, \vec{l}; q^0, \vec{q})^{ij}. \quad (305)$$

This gives

$$\begin{aligned} \frac{\pi(q)_{ab}^{ij}}{q^2} &= -g^2 \delta_{ab} \tilde{\mu}^{2\epsilon} \int \frac{d^{3-2\epsilon} \vec{l}}{(2\pi)^{3-2\epsilon}} \frac{2(|\vec{k}_+| + |\vec{k}_-|)}{2|\vec{k}_+| 2|\vec{k}_-|} \\ &\times \frac{N\left(\frac{1}{2}(|\vec{k}_+| - |\vec{k}_-|), \vec{l}; |\vec{k}_+| + |\vec{k}_-|, \vec{q}\right)^{ij}}{\vec{q}^2 (\vec{q}^2 - q^2)} \end{aligned} \quad (306)$$

where

$$\vec{q}^2 = (|\vec{k}_+| + |\vec{k}_-|)^2 - \vec{q}^2. \quad (307)$$

We will be interested in the  $q^2 \rightarrow 0$  limit of this, which is obtained by simply setting  $q^2 = 0$  in the factor  $1/(\vec{q}^2 - q^2)$  on the right hand side of the equation.

Consider this quantity at  $q^2 = 0$ . It is convenient to supply a factor  $1/(2|\vec{q}|)$ , the denominator factor for a cut propagator on one side of the self energy. Define  $\mathcal{G}_V$  by

$$\left[ \frac{1}{2|\vec{q}|} \frac{\pi(q)_{ab}^{ij}}{q^2} \right]_{q^2=0} = \frac{g^2}{(2\pi)^3} \mathcal{G}_V^{ij}, \quad \epsilon = 0. \quad (308)$$

Then  $\mathcal{G}_V^{ij}$  is the quantity that is included in the graph after extracting a conventional normalization factor  $\mathcal{N}$ . We have

$$\mathcal{G}_V^{ij} = -\delta_{ab} \frac{(|\vec{k}_+| + |\vec{k}_-|)}{|\vec{k}_+ + \vec{k}_-|} \frac{N\left(\frac{1}{2}(|\vec{k}_+| - |\vec{k}_-|), \vec{l}; |\vec{k}_+| + |\vec{k}_-|, \vec{q}\right)^{ij}}{2|\vec{k}_+| 2|\vec{k}_-| (\vec{q}^2)^2} \quad (309)$$

Note that this represents the sum of the graph in which the propagator following the self-energy is cut and the graph in which the propagator preceding the self-energy is cut.

The corresponding factor for the graph with the self-energy subgraph cut is

$$\mathcal{G}_R^{\mu\nu} = \delta_{ab} \frac{N\left(\frac{1}{2}(|\vec{k}_+| - |\vec{k}_-|), \vec{l}; |\vec{k}_+| + |\vec{k}_-|, \vec{q}\right)^{\mu\nu}}{2|\vec{k}_+| 2|\vec{k}_-| (\vec{q}^2)^2}. \quad (310)$$

Here we need not just the space-space components  $N^{ij}$ , but also  $N^{0j}$ ,  $N^{i0}$ , and  $N^{00}$ , since we do not have Eq. (291) to eliminate the components with  $\mu$  or  $\nu$  equal to 0.

When  $\vec{l}$  becomes collinear with  $\vec{q}$ , with  $\vec{l} \rightarrow (x - 1/2)\vec{q}$  with  $0 < x < 1$ , the virtuality

$$\vec{q}^2 = (|\vec{k}_+| + |\vec{k}_-|)^2 - |\vec{k}_+ + \vec{k}_-|^2 \quad (311)$$

approaches zero, so that there are divergences in the space-space components of the integrands (309) and (310). We can verify that there will be a cancellation of final state collinear singularities. First of all, the numerator factor  $N$  contains one factor  $\vec{q}^2$ , so that the divergences are only logarithmic. Given the infrared safety property of the measurement functions  $\mathcal{S}$ , the functions that multiply  $\mathcal{G}_V$  and  $\mathcal{G}_R$  are equal in the collinear limit. In the limit, the factor  $(|\vec{k}_+| + |\vec{k}_-|)/(|\vec{k}_+ + \vec{k}_-|)$  in the virtual graph approaches 1. Thus the collinear singularity cancels between the real and virtual graphs, and this cancellation occurs point by point in the integration over loop momenta.

We note, however, that the cancellation between  $\mathcal{G}_R^{\mu\nu}$  and  $\mathcal{G}_V^{\mu\nu}$  is not complete in the case of  $\mathcal{G}_R^{0j} v_j$  where  $\vec{v}$  is a vector orthogonal to  $\vec{q}$ . A singularity of the form  $\vec{l}_P \cdot \vec{v}/\vec{l}_P^2$  is left over, where  $\vec{l}_P$  is the part of  $\vec{l}$  orthogonal to  $\vec{q}$  as in Eq. (300). There is nothing that cancels this singularity because  $\mathcal{G}_V^{0j} = 0$ . The singularity is not too severe, but it is better to get rid of it. This can be arranged by providing a piece of  $\mathcal{G}_V^{\mu\nu}$  of the form

$$\mathcal{G}_V^{0j} = -\delta_{ab} \frac{\mathcal{Q}^2}{\vec{q}^2 + \mathcal{Q}^2} \frac{A_1 l_P^0 l_P^j}{2|\vec{k}_+| 2|\vec{k}_-| (\vec{q}^2)^2}. \quad (312)$$

The integral of this is zero because the integrand is odd under  $l_P^j \rightarrow -l_P^j$ . The factor  $\mathcal{Q}^2/(\vec{q}^2 + \mathcal{Q}^2)$  is 1 in the limit  $\vec{q}^2 \rightarrow 0$ , allowing the wanted cancellation, and provides convergence for large  $\vec{l}_P$ .

## 18.4 Renormalization

The integration in Eq. (306) is ultraviolet divergent and needs renormalization. We work by subtracting a suitably chosen integral from  $\tilde{\pi}^{ij}$ , which we will then relate to the  $\overline{\text{MS}}$  subtraction. We will subtract

$$\frac{\tilde{\pi}(q)_{ab}^{ij}}{q^2} = -g^2 \delta_{ab} \tilde{\mu}^{2\epsilon} \int \frac{d^{3-2\epsilon} \vec{l}}{(2\pi)^{3-2\epsilon}} \frac{\tilde{N}(\vec{l}, \vec{q})^{ij}}{16(\vec{l}^2 + M^2)^{5/2}}, \quad (313)$$

where

$$\tilde{N}(\vec{l}, \vec{q})^{ij} = (4N_c - 4N_f - 4N_c\epsilon) l_P^i l_P^j + [(8N_c - 4N_f) \vec{l}^2 + (6N_c - 4N_f) M^2] T(q)^{ij}. \quad (314)$$

Two properties of  $\tilde{\pi}^{ij}$  are important.

First, the integrand of  $\tilde{\pi}^{ij}/q^2$  matches that of  $\pi^{ij}/q^2$  for large  $\vec{l}$ . (The term proportional to  $M^2/(\vec{l}^2 + M^2)^{5/2}$  does not play a role in this property since the integrand behaves like  $|\vec{l}|^{-3}$  for large  $\vec{l}$  while this term goes to zero like  $|\vec{l}|^{-5}$ .) Thus the integral for

$$\frac{\pi(q)_{ab}^{ij}}{q^2} - \frac{\tilde{\pi}(q)_{ab}^{ij}}{q^2} \quad (315)$$

is analytic at  $\epsilon = 0$ . We can calculate this integral in three spatial dimensions, setting  $\epsilon = 0$ .

Second, it is easy to compute  $\tilde{\pi}^{ij}$ . The result is

$$\frac{\tilde{\pi}(q)_{ab}^{ij}}{q^2} = -\frac{\alpha_s}{4\pi} \frac{5N_c - 2N_f}{3} \delta_{ab} T(q)^{ij} \Gamma(\epsilon) \left( \frac{4\pi\tilde{\mu}^2}{M^2} \right)^\epsilon. \quad (316)$$

The term proportional to  $M^2/(\vec{l}^2 + M^2)^{5/2}$  in Eq. (313) does play a role here. Without it, the numerical factor  $(5N_c - 2N_f)$  would become  $(5N_c - 2N_f) - (3N_c - 2N_f)\epsilon$ , which would affect the finite part of the result as  $\epsilon \rightarrow 0$ .

We can now use these results. Expanding Eq. (316) about  $\epsilon = 0$ , we have

$$\tilde{\pi}_{ab}^{ij} = [\tilde{\pi}_{ab}^{ij}]_{\text{pole}} + [\tilde{\pi}_{ab}^{ij}]_{\text{R}} + \mathcal{O}(\epsilon). \quad (317)$$

The pole part is

$$[\tilde{\pi}_{ab}^{ij}]_{\text{pole}} = -\frac{\alpha_s}{4\pi} \frac{5N_c - 2N_f}{3} \delta_{ab} q^2 T(q)^{ij} \frac{1}{\epsilon}. \quad (318)$$

The renormalized  $\tilde{\pi}_{ab}^{ij}$  is

$$[\tilde{\pi}_{ab}^{ij}]_{\text{R}} = -\frac{\alpha_s}{4\pi} \frac{5N_c - 2N_f}{3} \delta_{ab} q^2 T(q)^{ij} \ln\left(\frac{\mu^2}{M^2}\right). \quad (319)$$

where the subtraction is according to the  $\overline{\text{MS}}$  renormalization prescription and where the  $\overline{\text{MS}}$  scale factor  $\mu$  is defined by  $\mu^2 = 4\pi\tilde{\mu}^2 e^{-\gamma}$ .

Let us write  $\pi_{ab}^{ij}$ , renormalized in the  $\overline{\text{MS}}$  prescription, as

$$[\pi_{ab}^{ij}]_{\text{R}} = \left\{ \pi_{ab}^{ij} - [\pi_{ab}^{ij}]_{\text{pole}} \right\}_{\epsilon=0}, \quad (320)$$

where  $[\pi_{ab}^{ij}]_{\text{pole}}$  is the same as  $[\tilde{\pi}_{ab}^{ij}]_{\text{pole}}$ , Eq. (318). Then we can use our results for  $\tilde{\pi}_{ab}^{ij}$  to write

$$[\pi_{ab}^{\mu\nu}]_{\text{R}} = \{ \pi_{ab}^{\mu\nu} - \tilde{\pi}_{ab}^{\mu\nu} \}_{\epsilon=0} + [\tilde{\pi}_{ab}^{\mu\nu}]_{\text{R}}. \quad (321)$$

This is convenient for calculation. The first term can be evaluated by numerical integration in three spatial dimensions. The second term is not conveniently calculated numerically, but it vanishes if we set

$$M^2 = \mu^2. \quad (322)$$

After extracting conventional normalization factors that contribute to  $\mathcal{N}$ , the factors that are included in the calculated quantity  $\mathcal{G}$  corresponding to the counter terms are given by

$$\left[ \frac{1}{2|\vec{q}|} \frac{\tilde{\pi}(q)^{ij}}{q^2} \right]_{q^2=0} = \frac{g^2}{(2\pi)^3} \tilde{\mathcal{G}}_V, \quad \epsilon = 0. \quad (323)$$

Here

$$\tilde{\mathcal{G}}_V = -\delta_{ab} \int d^3 \vec{l} \frac{(4N_c - 4N_f) l_P^i l_P^j + [(8N_c - 4N_f) \vec{l}^2 + (6N_c - 4N_f) M^2] T(q)^{ij}}{32|\vec{q}|(\vec{l}^2 + M^2)^{5/2}}. \quad (324)$$

## 19 Quark self-energy

In this section, we consider the quark self-energy subgraphs, including their renormalization.

### 19.1 Structure of the quark self-energy

There is one contribution to the quark self-energy  $\Sigma(k)$  at one loop. It has the form (with Dirac indices and color indices suppressed)

$$\Sigma(q) = \not{A}(q^2). \quad (325)$$

We will consider the quantity

$$\frac{\not{\Sigma}(q)\not{q}}{q^2} = \not{A}(q^2). \quad (326)$$

This quantity can be written as

$$\frac{\not{\Sigma}(q)\not{q}}{q^2} = ig^2 \tilde{\mu}^{2\epsilon} \int \frac{d^{4-2\epsilon} l}{(2\pi)^{4-2\epsilon}} \frac{N(l, q)}{q^2 [k_-^2 + i\epsilon][k_+^2 + i\epsilon]}, \quad (327)$$

where  $k_\pm^\mu = \frac{1}{2}q^\mu \pm l^\mu$  and, again,  $C_F = (N_c^2 - 1)/[2N_c]$  and  $\mu^2 = 4\pi\tilde{\mu}^2 e^{-\gamma}$ . The numerator function has the form

$$N = -C_F \not{\gamma}_\mu \not{k}_- \gamma^\mu \not{q} = 2C_F(1 - \epsilon) \not{\gamma}_\mu \not{k}_-. \quad (328)$$

## 19.2 Dispersive representation

We consider  $f(E) \equiv \not{\!q}\Sigma(q)\not{\!q}/q^2$  where  $E = q^0$ . This function is analytic in the  $E$  plane cut along the real axis from  $-\infty$  to  $-|\vec{q}|$  and from  $|\vec{q}|$  to  $\infty$ . Thus

$$f(E) = \frac{1}{2\pi i} \int_{|\vec{q}|}^{\infty} d\bar{E} \left\{ \frac{\text{disc}f(\bar{E})}{\bar{E} - E} - \frac{\text{disc}f(-\bar{E})}{\bar{E} + E} \right\} \quad (329)$$

We find for the discontinuity of  $f(E)$  for positive  $E$

$$\begin{aligned} \text{disc}f(\bar{E}) &= -ig^2 \tilde{\mu}^{2\epsilon} \int \frac{d^{3-2\epsilon} \vec{l}}{(2\pi)^{3-2\epsilon}} (2\pi) \delta(|\vec{k}_+| + |\vec{k}_-| - \bar{E}) \\ &\quad \times \frac{N\left(\frac{1}{2}(|\vec{k}_+| - |\vec{k}_-|), \vec{l}; |\vec{k}_+| + |\vec{k}_-|, \vec{q}\right)}{2|\vec{k}_+| 2|\vec{k}_-| \bar{q}^2} \end{aligned} \quad (330)$$

with  $\bar{q}^2 = (|\vec{k}_+| + |\vec{k}_-|)^2 - \bar{q}^2$ . The numerator function is simple. With  $k_+^2 = k_-^2 = 0$  we have

$$(\not{k}_+ + \not{k}_-) \not{k}_- (\not{k}_+ + \not{k}_-) = \not{k}_+ \not{k}_- \not{k}_+ = 2k_+ \cdot k_- \not{k}_+ = \bar{q}^2 \not{k}_+. \quad (331)$$

with  $k_+^0 = |\vec{k}_+|$ . Thus

$$\begin{aligned} \text{disc}f(\bar{E}) &= -ig^2 2C_F(1-\epsilon) \tilde{\mu}^{2\epsilon} \int \frac{d^{3-2\epsilon} \vec{l}}{(2\pi)^{3-2\epsilon}} (2\pi) \delta(|\vec{k}_+| + |\vec{k}_-| - \bar{E}) \\ &\quad \times \frac{|\vec{k}_+| \gamma^0 - \vec{k}_+ \cdot \vec{\gamma}}{2|\vec{k}_+| 2|\vec{k}_-|} \end{aligned} \quad (332)$$

For negative  $E$  we find

$$\begin{aligned} \text{disc}f(-\bar{E}) &= ig^2 2C_F(1-\epsilon) \tilde{\mu}^{2\epsilon} \int \frac{d^{3-2\epsilon} \vec{l}}{(2\pi)^{3-2\epsilon}} 2\pi \delta(|\vec{k}_+| + |\vec{k}_-| - \bar{E}) \\ &\quad \times \frac{-|\vec{k}_+| \gamma^0 - \vec{k}_+ \cdot \vec{\gamma}}{2|\vec{k}_+| 2|\vec{k}_-|}. \end{aligned} \quad (333)$$

Adding these according to Eq.(329), we get

$$\begin{aligned} \frac{\not{\!q}\Sigma(q)\not{\!q}}{q^2} &= -g^2 2C_F(1-\epsilon) \tilde{\mu}^{2\epsilon} \int \frac{d^{3-2\epsilon} \vec{l}}{(2\pi)^{3-2\epsilon}} \\ &\quad \times \frac{2q^0 |\vec{k}_+| \gamma^0 - 2(|\vec{k}_+| + |\vec{k}_-|) \vec{k}_+ \cdot \vec{\gamma}}{2|\vec{k}_+| 2|\vec{k}_-| (\bar{q}^2 - q^2)}. \end{aligned} \quad (334)$$

Consider this quantity at  $q^2 = 0$ . It is convenient to supply a factor  $1/(2|\vec{q}|)$ , the denominator factor for a cut propagator on one side of the self energy. Then we define  $\mathcal{G}_V$  by

$$\left[ \frac{1}{2|\vec{q}|} \frac{\not{\!q}\Sigma(q)\not{\!q}}{q^2} \right]_{q^2=0} = \frac{g^2}{(2\pi)^3} \mathcal{G}_V, \quad \epsilon = 0. \quad (335)$$

Then  $\mathcal{G}_V$  is the quantity that is included in the graph after extracting a conventional normalization factor  $\mathcal{N}$ . We have

$$\mathcal{G}_V = -C_F \int d^3 \vec{l} \frac{q^0 |\vec{k}_+| \gamma^0 - (|\vec{k}_+| + |\vec{k}_-|) \vec{k}_+ \cdot \vec{\gamma}}{2|\vec{q}| |\vec{k}_+| |\vec{k}_-| \vec{q}^2} \quad (336)$$

(Note that this represents the sum of the graph in which the propagator following the self-energy is cut and the graph in which the propagator preceding the self-energy is cut.)

For a subgraph in which neither the propagator following the self-energy nor the propagator preceding the self-energy is cut (so that  $q^2 \neq 0$ ), we can define

$$\left[ \frac{1}{q^2} \frac{\not{q} \Sigma(q) \not{q}}{q^2} \right] = \frac{g^2}{(2\pi)^3} \mathcal{G}_{VV}, \quad \epsilon = 0. \quad (337)$$

Then

$$\mathcal{G}_{VV} = -C_F \int d^3 \vec{l} \frac{q^0 |\vec{k}_+| \gamma^0 - (|\vec{k}_+| + |\vec{k}_-|) \vec{k}_+ \cdot \vec{\gamma}}{q^2 |\vec{k}_+| |\vec{k}_-| (\vec{q}^2 - q^2)}. \quad (338)$$

For a subgraph in which the self-energy part is cut, the corresponding factors are

$$\mathcal{G}_R = +C_F \int d^3 \vec{l} \frac{q^0 |\vec{k}_+| \gamma^0 - (|\vec{k}_+| + |\vec{k}_-|) \vec{k}_+ \cdot \vec{\gamma}}{2(|\vec{k}_+| + |\vec{k}_-|) |\vec{k}_+| |\vec{k}_-| \vec{q}^2}. \quad (339)$$

Note that here  $q^0 = |\vec{k}_+| + |\vec{k}_-|$ , so that the factors of  $|\vec{k}_+| + |\vec{k}_-|$  cancel between the numerator and the denominator. However, it is convenient to keep the numerator factor the same in each of these three cases. Note that the cancellation of collinear divergences between  $\mathcal{G}_V$  and  $\mathcal{G}_R$  is manifest in these formulas.

These formulas have been written in a form such that they work also for an antiquark propagator if  $q^\mu$  is chosen to be the momentum flowing in the quark direction. (Then in  $\mathcal{G}_R$  we have  $q^0/(|\vec{k}_+| + |\vec{k}_-|) = -1$ . The numerator is proportional to  $-|\vec{k}_+| \gamma^0 - \vec{k}_+ \cdot \vec{\gamma} = \not{k}_+$  with  $k_+^0 = -|\vec{k}_+|$ .)

### 19.3 Renormalization

The integration in Eq. (334) is divergent and needs renormalization. We will subtract

$$\begin{aligned} \frac{\not{q} \tilde{\Sigma}(q) \not{q}}{q^2} &= -g^2 \frac{C_F(1-\epsilon)}{4} \not{\mu}^{2\epsilon} \int \frac{d^{3-2\epsilon} \vec{l}}{(2\pi)^{3-2\epsilon}} \\ &\times \left\{ \frac{q^0 \gamma^0 - (2\vec{l} + \vec{q}) \cdot \vec{\gamma}}{(\vec{l}^2 + M^2)^{3/2}} + \frac{3(q^0 \gamma^0 - \vec{q} \cdot \vec{\gamma}) M^2}{2(1-\epsilon)(\vec{l}^2 + M^2)^{5/2}} \right\} \end{aligned} \quad (340)$$

Two properties of  $\tilde{\Sigma}$  are important.

First, the integrand of  $\not{q} \tilde{\Sigma}(q) \not{q}/q^2$  matches that of  $\not{q} \tilde{\Sigma}(q) \not{q}/q^2$  for large  $\vec{l}$ . (The term proportional to  $M^2/(\vec{l}^2 + M^2)^{5/2}$  does not play a role in this property since the integrand

has terms that behave like  $|\vec{l}|^{-2}$  and  $|\vec{l}|^{-3}$  for large  $\vec{l}$  while this term goes to zero like  $|\vec{l}|^{-5}.$ ) Thus the integral for

$$\frac{\not{q}\Sigma(q)\not{q}}{q^2} - \frac{\not{q}\tilde{\Sigma}(q)\not{q}}{q^2} \quad (341)$$

is analytic at  $\epsilon = 0.$  We can calculate this integral in three spatial dimensions, setting  $\epsilon = 0.$

Second, it is easy to compute  $\tilde{\Sigma}(q).$  The result is

$$\tilde{\Sigma}(q) = -\frac{\alpha_s}{4\pi} C_F \not{q} \Gamma(\epsilon) \left( \frac{4\pi\tilde{\mu}^2}{M^2} \right)^\epsilon. \quad (342)$$

The term proportional to  $M^2/(\vec{l}^2 + M^2)^{5/2}$  in Eq. (340) does play a role here. Without it, the numerical factor  $C_F$  would become  $C_F(1 - \epsilon),$  which would affect the finite part of the result as  $\epsilon \rightarrow 0.$

We use these results in the same way as in the gluon self-energy. Expanding Eq. (342) about  $\epsilon = 0,$  we have

$$\tilde{\Sigma} = [\tilde{\Sigma}]_{\text{pole}} + [\tilde{\Sigma}]_{\text{R}} + \mathcal{O}(\epsilon), \quad (343)$$

with

$$\begin{aligned} [\tilde{\Sigma}]_{\text{pole}} &= -\frac{\alpha_s}{4\pi} C_F \not{q} \frac{1}{\epsilon}, \\ [\tilde{\Sigma}]_{\text{R}} &= -\frac{\alpha_s}{4\pi} C_F \not{q} \ln\left(\frac{\mu^2}{M^2}\right). \end{aligned} \quad (344)$$

We can use our results for  $\tilde{\Sigma}$  to write

$$[\Sigma]_{\text{R}} = \left\{ \Sigma - \tilde{\Sigma} \right\}_{\epsilon=0} + [\tilde{\Sigma}]_{\text{R}}. \quad (345)$$

The first term can be evaluated by numerical integration in three spatial dimensions. The second term vanishes if we set

$$M^2 = \mu^2. \quad (346)$$

After extracting conventional normalization factors that contribute to  $\mathcal{N},$  the factors that are included in the calculated quantity  $\mathcal{G}$  corresponding to the counter terms are given by

$$\left[ \frac{1}{2|\vec{q}|} \frac{\not{q}\tilde{\Sigma}(q)\not{q}}{q^2} \right]_{q^2=0} = \frac{g^2}{(2\pi)^3} \tilde{\mathcal{G}}_V \quad \epsilon = 0. \quad (347)$$

and

$$\left[ \frac{1}{q^2} \frac{\not{q}\tilde{\Sigma}(q)\not{q}}{q^2} \right] = \frac{g^2}{(2\pi)^3} \tilde{\mathcal{G}}_{VV}, \quad \epsilon = 0. \quad (348)$$

Here

$$\tilde{\mathcal{G}}_V = - \int d^3\vec{l} \left\{ \frac{C_F}{8} \frac{q^0\gamma^0 - (2\vec{l} + \vec{q}) \cdot \vec{\gamma}}{|\vec{q}|(\vec{l}^2 + M^2)^{3/2}} + \frac{3C_F}{16} \frac{(q^0\gamma^0 - \vec{q} \cdot \vec{\gamma})M^2}{|\vec{q}|(\vec{l}^2 + M^2)^{5/2}} \right\} \quad (349)$$

and

$$\tilde{\mathcal{G}}_{VV} = \frac{2|\vec{q}|}{q^2} \tilde{\mathcal{G}}_V. \quad (350)$$

## References

- [1] R. K. Ellis, D. A. Ross and A. E. Terrano, Nucl. Phys. B **178**, 421 (1981).
- [2] Z. Kunszt, P. Nason, G. Marchesini and B. R. Webber in *Z Physics at LEP1*, Vol. 1, edited by B. Altarelli, R. Kleiss ad C. Verzegnassi (CERN, Geneva, 1989), p. 373
- [3] D. E. Soper, Phys. Rev. Lett. **81**, 2638 (1998) [hep-ph/9804454].
- [4] D. E. Soper, Phys. Rev. D **62**, 014009 (2000) [hep-ph/9910292].
- [5] D. E. Soper, *beowulf* Version 1.1, <http://zebu.uoregon.edu/~soper/beowulf/>.
- [6] D. E. Soper, *Beowulf 1.1 Technical Notes*, <http://zebu.uoregon.edu/~soper/beowulf/>.
- [7] Z. Kunszt and D. E. Soper, Phys. Rev. D **46**, 192 (1992).
- [8] G. Sterman, Phys. Rev. D **17**, 2773 (1978).